July 12, 2006

Chemical Sensor Networks for the Aquatic Environment

Kenneth S. Johnson,*† Joseph A. Needoba,† Stephen C. Riser,‡ and William J. Showers§

Monterey Bay Aquarium Research Institute, 7700 Sandholdt Road, Moss Landing, California, USA, School of Oceanography, University of Washington, Seattle, Washington, USA, Department of Marine, Earth and Atmospheric Sciences, North Carolina State University, Raleigh, North Carolina, USA

† Monterey Bay Aquarium Research Institute

‡ University of Washington

§ North Carolina State University

Contents

1. Introduction

This review focuses on chemical sensor networks that can be deployed on autonomous platforms in the aquatic environment and operated without significant human intervention for extended periods of time. The aquatic sensor networks that we consider have two essential characteristics; 1) chemical sensors are deployed at multiple locations, and 2) the networks are operated for months to years. We focus on observing systems that operate for extended periods for two primary reasons. Long-term observations of the environment are essential to understanding variability driven by natural and anthropogenic climate change. In situ sensors also provide the continuous data needed to characterize high frequency signals that cannot be easily sampled by manual methods. Under-sampling of time-varying environmental processes can result in aliasing of the observed signal. The variability that is driven by processes occurring at higher frequencies than the environment is sampled can appear as unrecognizable low energy events.[1]

Environmental chemists have often avoided the questions related to under-sampling time varying signals by assuming that aquatic systems are in a steady state. This has been necessary because, until the recent past, nearly all observations of chemicals in the aquatic environment have required that a sample be collected and returned to the laboratory where a variety of sophisticated tools can be used for sample analysis.[2] Much of the ocean is sampled only a few times in a decade because of the long (weeks in some cases) transit times from seaports to mid-ocean regions. Even in the

coastal ocean, or lakes and rivers, samples for chemical analysis are generally collected only at monthly intervals, if at all.[3] Such sampling rates are often inadequate to characterize dominant seasonal, daily or semi-diurnal processes. Even the signals of decadal-scale processes may be contaminated by variability that occurs at higher frequency. Interpretation of the linkages between processes is further obscured due to long-term lags between cause and effect.[4] As a result, we begin by arguing that observing the environment requires sustained observations at relatively high frequency.

1.1 The Sampling Problem

We illustrate the problems that arise in monitoring efforts that are based on manual sampling by considering nitrate in aquatic systems. Nitrate is the dominant source of fixed nitrogen for new plant growth in most aquatic ecosystems. Surface waters in the open ocean are depleted in plant nutrients, including nitrate. This depletion is a result of nutrient incorporation by photosynthetic organisms and subsequent sinking of organic material in fecal pellets and decaying organic matter. Deep waters are enriched in nutrients when bacteria remineralize the sinking particles. The low concentrations of nitrate in the sunlit surface waters limit the accumulation of plant biomass in many marine and freshwater systems.[5] The vertical mixing of essential nutrients from deep waters into the sunlit euphotic zone then becomes the rate-limiting step for primary production of new organic carbon.

Figure 1 shows nitrate measurements made on a mooring located 20 km off the central California coast at hourly intervals for one year[6] using an optical nitrate sensor[7] and nitrate measurements in samples collected near the mooring at ~21 day intervals. The annual cycle observed by the moored chemical sensor shows a series of events throughout the year with high (>10 μM) nitrate concentrations. These events are produced by upwelling of cold, nutrient rich water, which is driven to the surface when the wind blows to the southwest in this region. Upwelling of cold, nutrient-rich deep water into warm, nutrient-poor surface water produces the anti-correlation in temperature and nitrate (Figure 1). The nutrients carried into sunlit surface waters during the upwelling events result in phytoplankton blooms that increase chlorophyll concentrations and deplete nitrate (Figure 1). This cycle of events, clearly seen in the hourly data, is not easily resolved in monthly monitoring data. A quantitative understanding of such processes has come from intensive field sampling campaigns. However, intensive field programs are difficult to sustain in the long-term. As a result, most aquatic environments are severely under-sampled, long-term variations are not understood, and our understanding of environmental processes can be quite biased.

In addition to large temporal variability, there is also significant spatial variability in concentrations of chemicals that play important roles in regulating ecosystems. For example, the physical processes that reintroduce nutrients to the surface have high spatial variability. This may produce great spatial variability in the growth of phytoplankton populations. Thus, chemical sensors in this type of environment should, ultimately, be capable of characterizing high spatial variability, as well as temporal variability.

The under-sampling problem, which is inherent in measurement programs that are based on manual sample collection, can be overcome by either using remote sample collection devices[8, 9] or by making nearly continuous chemical measurements over long time periods on networks of unattended platforms. Here we focus on systems that make in situ measurements. Chemical sensors deployed in situ for extended periods have shown the impacts of events driven by storms,[10] eddies,[11, 12] El Niño climate oscillations,[13, 14] planetary (Rossby) waves,[15] tides,[16] upwelling,[6] and ice melting.[17]

1.2 Data at Global Scales

The need for a better understanding of the linkages between chemicals and environmental processes is being driven by the scope of environmental change presumed to be occurring around the planet. During the past 100 years, concentrations of carbon dioxide in the atmosphere have increased 36%, industrial and agricultural processes that fix dinitrogen gas have grown to the point where their rates now exceed natural processes,[18] some 10 to 50% of the photosynthetic products on land are appropriated by processes controlled by humans,[19] and one half of the accessible freshwater runoff is already utilized.[20] Such global scale processes necessarily require global observing systems.

The best example of the power of a global environmental chemical analysis network is the system of stations that collect atmospheric measurements of carbon

dioxide and oxygen. These networks build on the pioneering work of the late Charles David Keeling, who started the time series of atmospheric carbon dioxide measurements at Mauna Loa in Hawaii. Keeling's CO_2 data from Mauna Loa have played a seminal role in identifying human perturbation of global chemical cycles and it has been the most influential environmental data set now available. His results led to an expansion of the observing system and there is now a network of stations around the world where samples for carbon dioxide and oxygen are collected.[21, 22] The network measurements reveal distinct annual cycles in atmospheric oxygen and carbon dioxide concentrations. Further, there is a distinct geographic pattern to the variability that is related to differences in land and ocean areas in the Northern and Southern Hemispheres. The patterns of annual variation are driven by photosynthesis and respiration on land and in the sea and by differences in the rates at which these two chemicals equilibrate across the air-sea interface. These geographic and temporal variations in chemical properties of the atmosphere allow the long-term, network-based observations to be used to create estimates of global net primary production on land and in the ocean and to quantify the inter-annual change in these rates.[21, 22]

Ultimately, monitoring the aquatic biogeochemical cycles and their impacts on the environment and climate will require dense networks of chemical sensors that operate at global scales within the oceans, lakes and rivers, as well as in the atmosphere. While there are no direct examples operating at a global scale today, there are a variety of in situ chemical sensor networks operating at smaller scales. Further, there are examples of global aquatic sensor networks that illustrate the potential for the development of

networks that sense chemical properties. For example, we describe in Section 3.2 chemical sensors measurements from the Argo array of profiling floats.[23] These platforms have become an important tool for observing the large-scale ocean circulation. Profiling floats typically drift passively with the flow at depths of 1000 or 2000 m in the ocean and then cycle at 7 to 10 day intervals between their parking depth by inflating an external bladder, which increases float volume without changing mass. This causes the float to rise. During the ascent to the surface, the floats collect measurements of oceanic variables such as temperature and salinity at 50-75 different pressure levels. The floats transmit their data to an orbiting satellite while on the surface and then descend back to their parking depth to begin another cycle.

A map of seawater salinity at a depth of 200 m based on in situ salinity measurements that were made by ~1200 Argo floats in the Pacific Ocean during the first two weeks of December 2005 is shown in Figure 2 (35 on the IAPSO Practical Salinity Scale[24] is nearly equal to 35 g salt/1000g seawater). The program OceanDataView[25] was used to read the data and create the map. The Argo array illustrates the potential for operating global sensor networks within the aquatic environment. Further, profiling floats are now being equipped with chemical sensors.[26]

The Argo array is building to a sustained set of 3000 floats, approximately one per each 3 degree longitude by 3 degree latitude box in the ocean. Given the richness of biological and chemical processes, which produce distributions with greater complexity than temperature or salinity, we will need sensor arrays with equivalent, if not greater

sampling density, to be able to resolve important biological processes in the ocean. On continents, one might expect that chemical sensor networks designed to monitor transport of nutrient elements from land to the coastal ocean would require sampling densities similar to that used to assess water flow in streams. There are presently some 3600 real-time stations operated by the United States Geological Survey to monitor stream flow in the USA.

2. In Situ Chemical Sensors and Analyzers

There has been an extensive effort to design chemical sensors and analyzers that are capable of operating in situ. Much of this work has been recently summarized in two volumes on chemical sensor systems for aquatic sciences.[27, 28] In addition, in situ electrochemical sensors have been reviewed,[29] as were chemical and biological sensors for time-series research.[30] The two volumes contain chapters that describe a variety of continuous flow analyzers, electrochemical sensors and optical sensors for in situ measurements of dissolved chemical species. Most of this work remains focused on the research required to develop prototype sensor systems and relatively few chemical sensors are available that are robust enough for routine and widespread use in networks. Here we focus on chemical monitoring systems that have matured to the point where there are data records from instruments deployed in the field for at least one to two months.

Why are autonomous chemical sensors not in broader use? The scarcity is related to the analytical challenge in making autonomous chemical measurements in natural waters with complex background matrices against which low analyte concentrations must be detected. In the laboratory, these analytical challenges can be overcome through the use of very sophisticated instrumentation. These complex measurements often involve several analytical steps and are the so called hyphenated methods: for example, gas chromatography-mass spectrometry, organic extraction-graphite furnace atomic absorption spectrophotometry, and isotope dilution-high resolution inductively coupled plasma-mass spectrometry.[2] While a number of laboratories have developed portable instrumentation based on sophisticated methods such as ICP-MS,[31] they still require frequent operator attention and, in many cases, they require a portable laboratory on site to provide power and clean working spaces. In situ chemical sensors or analyzers that can be deployed in network arrays for long time periods require much simpler and more robust methods of chemical analysis.

A variety of approaches have been used to monitor chemicals in situ. Most familiar are sensor systems in which the sample interacts directly with the sensor without additional chemical manipulations. These include electrochemical sensors such as membrane-covered Clark oxygen cells[32] and pH electrodes. A variety of more sophisticated sensors based on electrochemical analyses are now possible,[29] which enable studies of chemical speciation in unique environments.[33] Direct optical chemical sensors are also becoming more common. Fluorescence quenching sensors based on immobilized platinum and ruthenium complexes are available for measurement of

oxygen.[34, 35] Spectrophotometers can be used in situ for the direct determination of nitrate and sulfide using their distinctive ultraviolet absorption spectra.[7, 36] All of these instruments must either be extremely stable or capable of self-calibration[37] in order to produce quality data over long periods of time.

One of the major challenges to operation of chemical sensor systems is biofouling of sensor surfaces. In highly productive coastal and estuarine waters, sensor surfaces may be overgrown by organisms within a few weeks (Figure 3). The biofouling organisms may create microenvironments that alter chemical concentrations, block optical paths and create barriers to the flow of chemicals to sensing surfaces. A variety of methods have been adapted to mitigate the effects of biofouling.[38, 39] However, none has proven universally successful and each system requires empirical assessments to find effective methods.

Simple sensor systems that are immune to fouling, capable of operating without drift for long periods of time, and sufficiently selective and sensitive are not yet available for most chemical species of interest in the aquatic environment. As a result, in situ chemical monitoring often requires more complex instrumentation, which is used to perform multi-step chemical analyses in the same manner as the familiar continuous flow analyzers that are used on board ship. These instruments generally require more complex apparatus with pumps, valves, fluidic manifolds, separate detectors, reagent reservoirs and highly trained operators. These analyzers are often based on the principles of Flow Injection Analysis.[40] Reviews[41, 42] describe a variety of these in situ analysis systems.

In the following sections, we describe the chemical sensors that have been deployed in situ, in lakes, rivers or the ocean and which have data records that extend over periods of at least a few months. Given the long time frames required to bring chemical analysis systems to this level of maturity, these sensors are likely the main candidates for deployments in the next generation of chemical sensor networks. We then describe examples of the networks that are now operating and which use these sensors or analyzers.

2.1. Dissolved Gases other than CO_2

A variety of sensors exist for dissolved oxygen, total gas pressure, and methane that have demonstrated endurances in excess of a month while deployed in situ. Sensors for dissolved gases, particularly oxygen, are probably the most widely used of chemical sensors in aquatic environment.

2.1.1 Dissolved Oxygen

Oxygen sensors are of particular interest because of the role of oxygen in metabolism. The dissolved oxygen concentration is an indicator of primary production of fixed organic material and respiration of organic carbon.[43] The depletion of oxygen below critical levels is lethal to animals.[5, 44] Oxygen sensors based on a membrane covered, amperometric electrode (the Clark electrode[32]) are probably the most common

chemical sensor system used in the aquatic sciences. They are routinely used on conductivity-temperature-depth-O_2 ($CTDO_2$)/rosette sampler packages that are lowered from ships to collect water and measure the vertical distribution of temperature, salinity, and oxygen. Handheld oxygen sensors are often used for spot monitoring of inland waters.

Biofouling in productive environments can require that Clark oxygen sensors be cleaned or replaced at weekly intervals when they are continuously deployed.[45] Monthly recalibration is required even in very low productivity regions of the upper ocean.[46] As a result, there are not large numbers of long-term records from Clark oxygen electrodes in the aquatic environment, although they are becoming more common as solutions to the biofouling problem are developed. The effects of biofouling on Clark electrodes tend to be least severe in lakes and they have been used in long-term studies of primary production under ice in northern lakes.[17] In estuaries and the ocean, the applications include studies of gas exchange[10] and respiration and primary production[46, 47] during long-term deployments.

Deployment of oxygen electrodes on vertically profiling platforms, such as floats[23] and gliders,[48] greatly alleviates the fouling problems in marine environments. These platforms spend a substantial fraction of time at depths below the euphotic zone in waters where biofouling is not severe. For example, consider results obtained with the first profiling float equipped with a modified Seabird Electonics SBE43, which is a membrane-covered Clark oxygen electrode. This float was deployed as part of the Argo

array (University of Washington float 0894) near the Hawaii Ocean Time series (HOT) station[49] at 22.75°N, 158°W in August of 2002. Float 0894 drifted at a depth of 1000 m and profiled to the surface at 10-day intervals for nearly 3 years, reporting more than 100 oxygen profiles. Before every fourth profile, the float descended to a depth of 2000 m and then rose to the sea surface. As can be seen in Figure 4, float 0894 remained in the vicinity of the Hawaiian Islands for most of its 3-year drift, only breaking away to the west during its final 10 profiles. This allows meaningful comparisons to be made with monthly shipboard measurements at the HOT station.

A profile of float 0894 from 2000 m to the surface (Figure 5) shows the typical distribution of temperature, salinity, and dissolved O_2 in the North Pacific. All three variables take on their maximum values near the sea surface. Temperature decreases monotonically from the surface to 2000 m. Salinity and dissolved O_2 show a decrease in the upper ocean with a mid-depth minimum near 500 m for salinity and 800 m for dissolved O_2. The subsurface O_2 minimum is due to a balance between O_2 inputs from the atmosphere and biological production at the sea surface, and its loss by respiration in the ocean interior. High oxygen concentrations in the deepest water are produced by the high solubility of oxygen in cold water masses that sink from the surface in polar oceans and spread into the deep basins. Measurements are made at 71 different pressure levels (note that the pressure at the bottom of a 1 meter column of seawater is almost exactly 1 decibar, so that the depth given in meters and pressure in decibars are essentially interchangeable numerically) and the vertical distributions of each property are well resolved.

There is a seasonal cycle in dissolved O_2 concentration measured at the sea surface near the HOT site (Figure 6a). This cycle is primarily controlled by the seasonal cycle of sea surface temperature and the temperature-dependent solubility of O_2 in seawater. The O_2 solubility at the sea surface is highest during the winter, when the sea surface temperature is a minimum. The O_2 concentration steadily increases early in the year as atmospheric O_2 equilibrates with surface water. As the temperature rises in the spring, the water becomes supersaturated with O_2, and by late spring or early summer dissolved O_2 is removed from the surface waters by outgassing to the atmosphere. This seasonal cycle is seen in both the HOT shipboard O_2 station data, which is collected at the same site each month, and the surface data from profiling float 0894 (Figure 6a).

While the temporal variability in the shipboard and float O_2 observations is similar, the actual measured values of dissolved O_2 in the two datasets differ consistently by about 5 μmol/kg (a 2.5% offset), with the shipboard values usually higher. Since the shipboard values are determined manually from a highly accurate Winkler titration,[50] they are presumed to be correct. The offset is roughly consistent with the manufacturer's specifications for the SBE oxygen sensor of initial accuracy of 2% of the saturation value. A similar finding emerges for the deep water: there is no systematic divergence over ~3 years time at 2000 m between the shipboard measurements and those collected from float 0894 (Figure 6b). This again suggests a calibration offset on the float sensor, but again the lack of systematic sensor drift over 3 years is highly encouraging. This is

an important finding and bodes well for the use of such sensors on profiling floats, where the sensor is unattended for periods of 5 years or more.

The problems created by biofouling have led to considerable effort to develop even more robust oxygen sensors based on alternative technologies. Oxygen quenching of fluorescent compounds containing metal ions such as ruthenium or platinum is one extremely promising technology.[51] Fluorescence sensors do not consume oxygen and they are less sensitive to fouling that alters the diffusion rate of oxygen through the membrane. At least three commercial products using this principle are now available for in situ measurements. Fluorescence-based sensors respond to oxygen partial pressure, as opposed to oxygen concentration in electrode systems. The fluorescence quenching is generally not linear, which makes calibration somewhat more complicated in these systems. Fluorescence-based systems may also suffer long term drift due to photo-bleaching of the dye and leaching of the dye from the matrix used to immobilize it.[51] Robust, long-term deployments have required systems that use fluorescence life-time measurement methods. Lifetime measurements are nearly immune to loss of the fluorophore due to photo-bleaching or other processes when compared to direct detection of fluorescence intensity. Lifetime-based fluorescence quenching oxygen sensors have been deployed for time periods in excess of one year with no significant drift.[35, 52] For example, measurements of dissolved oxygen in the North Atlantic Ocean were made over a time period of 600 days on a profiling float of the type described above (Figure 7).[35] Measured oxygen concentrations at a depth of 1800 m, where little change was expected, averaged 295.0±0.7 (1 standard deviation) µM over the entire period. Further, some of

the change appears to be related to changes in water mass properties, identified by independent observations of density (Figure 7). These results suggest that oxygen measurements with a precision near 0.1% may be attainable over time periods greater than one year. Such capability would enable completely new methods of observing primary production and respiration in the ocean, lakes and rivers.

In addition, it is now possible to utilize novel waveforms in voltammetric sensors to measure oxygen without using membranes to protect the electrodes from fouling.[53] Unprotected electrodes may have a variety of advantages, particularly a faster response rate.[54] Better response rates will be key to utilization of oxygen sensors for applications such as the long-term measurements of oxygen flux into sediments by the eddy-correlation method.[55]

2.1.2 Methane and Total Gas Tension

The gas tension device (GTD) uses a rigid, gas permeable membrane and a stable, high precision pressure sensor to determine the total pressure exerted by dissolved gases.[56] The signal detected by the GTD is dominated by N_2 and O_2 in natural waters. If oxygen measurements are available, then its contribution can be subtracted from the total gas tension to yield the N_2 partial pressure.

GTD instruments are available commercially and have been successfully used on long-term ocean mooring deployments to deconvolve the various processes that may

change gas concentrations.[46] For example, oxygen saturation may increase due to biological oxygen production or due to seasonal warming that reduces the oxygen solubility with no actual change in concentration. Seasonal warming will also increase the percent saturation of dinitrogen gas. Parallel increases in oxygen and dinitrogen gas saturation are, therefore, indicative of warming, rather than biological production. Oxygen and GTD sensors has been used on open ocean moorings at the HOT station near Hawaii to compute primary production rates after correcting the observed changes in oxygen for the effects of seasonal warming that were estimated from changes in the degree of N_2 saturation.[46] These instruments have very good, long-term stability, albeit a slow response time that is required for gas to diffuse across the rigid membrane. Efforts are underway to adapt GTD's for oxygen sensing by scrubbing oxygen inside the instrument.

Methane is of considerable interest in aquatic sciences because of its heat trapping properties in the atmosphere and the role that methane hydrates may play in regulating production of methane in the ocean.[57] Methane sensors are commercially available that utilize a rigid, gas permeable membrane to separate gases from water and a semiconductor methane sensor to measure concentration in the gas phase. The systems have been used for a variety of studies, including long-term measurements of methane in ground water entering the coastal ocean.[58] The rigid membranes required for high pressure applications also limit the response rate of these sensors to ten's of minutes.

2.2 Inorganic Carbon System

Understanding the long-term variation in the mass of anthropogenic carbon dioxide stored within the ocean, the fluxes of CO_2 across the air-sea interface, and the rates of biological processes that move carbon to the deep sea are leading challenges in biogeochemistry. Complete characterization of the dissolved, inorganic carbon system requires measurement of two independent carbon dioxide parameters and a thorough understanding of the thermodynamic equilibria for acid/base chemistry in the solution under study. The parameters measured in the laboratory include the partial pressure of carbon dioxide in solution (pCO_2), pH, total inorganic carbon (TCO_2) or titration alkalinity (TA).

2.2.1 CO_2 Partial Pressure (pCO_2)

The partial pressure of CO_2 gas dissolved in water is currently the only inorganic carbon parameter that is regularly measured in situ for long time periods. A variety of optical sensors have demonstrated high quality pCO_2 measurements with endurances of many months on moorings and drifting buoys.[14, 59, 60] In order to be broadly useful, these methods must have an accuracy of 1 ppm pCO_2. Several methods for pCO_2 measurement are based on equilibrating seawater carbon dioxide across a gas-permeable membrane with a solution containing an acid-base indicator dye.[61, 62] The pCO_2 is then determined from the absorption spectra of the acid and base forms of the indicator dye. Response rate may be limited to 30 minutes or more if transport is entirely by diffusion.[62] To

overcome slow response rates, a pump may be used to periodically flush the optical path and refresh the indicator solution.[61]

Combining information from sensors for several chemicals can be especially useful for interpreting the biogeochemical processes in aquatic systems. [17, 59] Figure 8 shows a 3.5 month time series of measurements of pCO_2 and dissolved oxygen at two depths in a small lake that was initially ice covered.[17] The combination of multiple sensors at several depths showed a surprising series of events during the spring ice melt. The vertical gradient in chemical properties disappeared before ice melted in late April (Figure 8). This indicates convective overturn of the water column. These convective processes could not be easily observed with more traditional temperature measurements as the water column was nearly isothermal. The initial overturning was followed by a period of vertical mixing events that supplied large amounts of nutrients to the sunlit waters under the ice, resulting in high primary production rates. These processes have not been observed in programs based on manual sampling.

Direct measurements of the carbon dioxide mole fraction difference between the atmosphere and seawater, from which $\Delta pCO_2 = pCO_2$[seawater] – pCO2[air] is calculated, have been made using dual-beam infrared (IR) gas analyzers on moorings.[63] In this system, carbon dioxide dissolved in seawater is equilibrated with an isolated gas volume using wave energy to provide mixing in the equilibrator. The IR analyzer then measures the absorbance difference between one optical cell filled with gas quilibrated with surface seawater and one cell filled with ambient air. The equilibrator cell is

periodically filled with ambient air to calibrate the offset between the two beams. Measurements of ΔpCO_2 using this method have been made continuously for year-long time intervals on several of the TAO/TRITON moorings in the equatorial Pacific.[13] A similar system, combined with a Clark oxygen sensor, has been used for shorter periods to examine the processes that control net ecosystem metabolism in a large number of northern lakes.[64] Instruments based on measurements in the gas phase are generally limited to deployments within a few meters of the sea surface.

2.2.2 pH and Other Inorganic Carbon Properties

To fully characterize the state of inorganic carbon dissolved in seawater, which would allow calculation of carbonate and bicarbonate concentrations, one additional CO_2 system parameter must be measured. Seawater pH measurements with glass potentiometric electrodes are most familiar. While significant improvements have been made in the endurance and stability of pH electrodes, there remain significant issues with drift and stability during pressure and temperature variations. There are few long-term studies with potentiometric pH sensors that have yielded useful data in natural waters. Measurements of pH using optical measurements with pH sensitive dyes have generally replaced electrode measurements for high precision, shipboard studies.[65] In situ pH measurements using spectrophotometric procedures are now being made on an experimental basis.[66] Measurements of TCO_2 and TA with in situ analyzers are still in development.[67]

2.3 Nutrients

Measurements of dissolved plant nutrients (e.g. nitrate, ammonium, phosphate, orthosilic acid/dissolved silicate ion) are an essential component of most biogeochemical studies. The availability of these nutrients is the proximal control of primary production in most aquatic environments.

2.3.1 Nutrient Analyzers

A variety of adaptations of the standard colorimetric methods[68] for nitrate (reduction on cadmium to nitrite and determination as an azo dye), phosphate and silicate (as reduced molybdate dyes) have been developed for in situ analyses. These systems operate as continuous flow systems[69, 70, 71] similar to an unsegmented continuous flow analyzer or as batch analyzers.[16] Several of these instruments are available commercially. The basic hardware in these systems consists of pump, valves, fluidic manifold and a colorimetric detector. These components can be assembled in a variety of ways and, with relatively minor modifications, it is possible to use one set of hardware for a variety of analyses. Systems that use osmotically powered sample and reagent pumps,[69] requiring no external power source, have been adapted for year-long measurements of iron in hydrothermal vent systems at depths in excess of 2000 m.[72] Most systems are designed to be recalibrated in situ at periodic intervals by substituting a blank and standard for the sample. [41, 42] This can be done with stream selection valves or with individually selectable pumps for each solution.

To date, most of the published, long-term measurements in situ analyzer systems have focused on nitrate. Colorimetric nitrate analysis systems have been deployed in the open ocean for up to 4 month periods. These systems have been used to demonstrate the impacts of eddies[11] and planetary (Rossby) waves[15] on the upward transport of nutrient from deep water into the euphotic zone, and the subsequent impact on the phytoplankton community (Figure 9). In the coastal zone, moored nitrate analyzers have been used to study vertical nutrient transport by internal waves,[73] and the impact of lateral nutrient flux through estuaries[70, 74] and through the North Sea.[75] Colorimetric nutrient analyzers have been primarily deployed from piers or moorings. Size, power, complexity and cost would all impact the feasibility of long-term deployments on other types of platforms such as profiling floats.

2.3.2 Ion Selective Electrodes

Ion selective electrodes have not often been used widely on autonomous observing systems because of the difficulty in keeping systems in calibration and because they often lack sufficient specificity in marine systems with high salt backgrounds.[76] Monitoring systems that utilize ion selective electrodes for long time periods generally include a capability for autonomous recalibration of the system every few hours.[76] However, new sensor membranes are being developed with improved performance. For example, a new nitrate electrode system using N,N,N-triallylleucine betaine chloride immobilized in a polymer membrane has been developed that exhibits long-term

(months) stability.[77] Diurnal nitrate variations were found over a two-month period with this electrode during low flow conditions in the River Taw, in the southwest United Kingdom.[78] These diurnal concentration changes were subsequently verified with an intensive 90-hour discrete sampling program. In the Danube River, continuous hourly measurements of nitrate concentrations over an 11 month period with ion selective electrodes recorded weekly concentration variations below the Vienna, Austria waste water treatment plant that were 50% of the mean values.[79] Ammonium concentrations show daily variations that were 100 % of the mean concentration value, with "spot events" or spills that were 300% higher than the mean NH_4 concentration values.

2.3.3 UV Optical Nitrate Sensors

Recent developments in opto-electronics now make it possible to measure nitrate in seawater directly using its UV absorption spectrum.[7, 36] Such measurements require no chemical manipulations and will greatly extend the feasibility of routinely monitoring nitrate. The optical systems require approximately 5 to 10 W for continuous operations, but operation on a reduced duty cycle of about 3 seconds per complete measurement cycle makes year-long deployments feasible.[6] A significant issue with all long-term deployments is the ability of the sensor system to remain in calibration over long-term deployments. Nutrient analyzers solve this problem by carrying blank and standard solutions on board and periodically substituting these solutions for the sample. UV optical sensors can solve this problem by measuring the absorption spectrum with high

resolution. The spectrum contributed by fouling is nearly linear and can be deconvolved from the absorption signals due to nitrate and other UV-absorbing compounds.

Long-term deployments of optical nitrate sensors have been used to calculate daily changes in primary production.[6] Hourly measurements of nitrate on moorings show a diel cycle in nitrate concentration that is created by daytime uptake of nitrate during photosynthesis and restoration at night by physical processes (Figure 10). These changes in nitrate can be used to estimate the rate of carbon uptake and incorporation into living particles because the ratio of nitrogen to carbon in phytoplankton is nearly constant. The daily estimates of primary production from nearly three years of autonomous nitrate measurements show a consistent seasonal variability that is regulated by the rate of upwelling (Figure 10d).

2.4 Empirical Sensors

There are empirical relationships between sensed properties and chemical concentration that can be used to determine the distribution of chemicals in space and time. For example, it has been shown that there is a relatively constant proportionality between light scattering detected with a transmissometer and the concentration of particulate organic carbon (POC) in seawater.[80] The proportionality occurs in open ocean waters because there are few sources of particles other than in situ production by phytoplankton. This correlation has been used to make long-term observations of POC with transmissometers on profiling floats in the North Pacific[81] and Southern Ocean.[82]

These measurements have been used to monitor production of phytoplankton biomass following soil-aerosol deposition events in the North Pacific that release phytoplankton from iron-limitation.[81]

3. Chemical Sensor Networks

Considerable work is underway to develop environmental sensor networks.[83, 84] In this section we present examples of chemical sensor networks that have been operated in the aquatic environment for periods of at least one month with sensors at multiple locations. There are many challenges in building a network beyond that of developing and operating the sensor for extended periods. These challenges include providing a platform on which to deploy the sensor,[23, 85] providing power and communications,[86] and controlling biofouling.[38] Operating a complete network involves much greater complexity than chemical analysis alone. However, here we focus only on chemical sensing.

Most of the systems with chemical sensors that are now in place are focused around oxygen sensors, which are deployed in lakes,[83 , 85] estuaries, [84, 87] or coastal waters[88] to address water quality issues that result when oxygen is depleted in eutrophic environments. In the following, we focus on a set of examples that illustrate the next challenges in chemical sensor deployment as we move beyond oxygen sensor deployments in environments that are relatively accessible. These examples emphasize

sustained observations in difficult environments. Much of this work is based on newly developed capabilities.

3.1. MBARI/NOAA pCO_2 array

In section 2.2.1, we described the technology that can be used for measurements of the sea-air pCO_2 difference. Measurements of ΔpCO_2 in surface seawater represent the longest record of autonomous, chemical measurements in the marine environment. Measurements on moorings in Monterey Bay began in 1997 and extend through the present.[14] These long-term measurements allow the effects of infrequent events on carbon dioxide transfer from the air to the sea, such as the El Niño/La Niña climate oscillations, to be assessed in coastal[14] and open ocean environments.[13] The pCO_2 of recently upwelled water is generally very high because respiration of organic carbon in sinking particles releases carbon dioxide into the deeper waters. As a result, pCO_2 is high in the equatorial upwelling zone and in recently upwelled water of the eastern boundary currents along the US west coast. However, during El Niño events, reversals in wind direction along the equator send warm water as a Kelvin wave from the western to the eastern Pacific and then poleward along the continents.[13] This warm water deepens the thermocline and, although upwelling favorable winds continue along the California coast, the upwelled water does not have elevated carbon dioxide concentrations. Chemical sensor measurements on moorings off the California coast show that these effects reach the Monterey Bay region and appear as an annual period with no large increases in surface pCO_2 during El Niño years (Figure 11).[14] Such processes can alter the air-sea

transfer of carbon dioxide by large amounts. In collaboration with NOAA scientists, this network has been extended to include moorings throughout the Pacific Ocean that are operating in real-time (Figure 12).

3.2. Trans-Pacific Sections of Dissolved O_2 Measured on Argo Profiling Floats

The largest sensor network now operating autonomously in the ocean is the Argo array of profiling floats.[23] As discussed above, Argo is primarily an experiment designed to map the fields of oceanic temperature and salinity over the globe in order to determine the ocean's role in the global balance of heat and freshwater. The float array enables decadal-scale changes in these fields, which are driven by climate change, to be directly observed. In recent years, some floats have been equipped with dissolved O_2 sensors. The goal of this work is to examine sensor performance over times of a few years and to begin to plan future efforts, where the issue of carbon cycling and its relation to climate is likely to be more prominent.

As discussed in Section 2.1.1, profiling floats have been deployed using both optical sensors (the Aanderaa Optode)[35] and electrochemical, Clark-cell[89] sensors. Deployments on floats have demonstrated advantages and disadvantages to each of these sensor types. Optode sensors on floats have proven to be extremely stable over times of a year or more (Figure 7).[26, 35] Electrochemical O_2 sensors on floats, manufactured by SeaBird Electronics (SBE), have exhibited more variation. Very little drift has been seen with some sensors over times of several years (Figure 6b), but the mean drift for a large

number of sensors is greater than that observed with the Optode sensors, as we discuss below. The Clark cell, however, uses considerably less power in a float configuration than the Optode, an important issue since floats must function unattended over times as long as 5 years. At this point in time, the Argo community is actively exploring the optimal sensor configuration.

In late 2005, a line of 22 University of Washington Argo floats equipped with SBE dissolved O_2 sensors was deployed across the South Pacific Ocean, as shown in Figure 13a. This was the first attempt at deploying such a large number of floats with O_2 sensors at one time for the purpose of examining the variability of dissolved O_2 over basin scales. All of the floats were parked at a depth of 2000 m and profiled to the surface at 7-day intervals. A trajectory of one of the floats (Figure 13b) shows typical motions at 2000 m in this portion of the world ocean: the most prominent features are transient motions (eddy variability) that are usually several times larger than the weaker mean circulation. These currents dispersed the float array weakly over the course of several months.

The O_2 sensor drift for each of the 22 South Pacific floats was estimated from the measured oxygen at 2000 m for each profile, minus the initial 2000 m O_2 value (in order to remove the initial offset) (Figure 14). The results indicate that the drift over the first 18 profiles for 20 of the 22 floats ranged from ~0 to 10 μmol/kg towards lower values, a relative change of 0 to 6% (somewhat above the manufacturer's specification). The two exceptions were floats 2340 and 5025 (Figure 14); the erratic drift in the oxygen

measurements reported by these two floats results suggests major O_2 sensor problems. For 20 of the 22 floats deployed (>90%), the SBE O_2 sensors performed reasonably well. These results illustrate one of the strengths of a sensor network. Unreliable sensors can often be identified if they exhibit behavior that is inconsistent with other members of the array.

Data from the first 150 days after deployment are shown for one sensor deployed on float 2348 (Figure 15), whose trajectory is shown in Figure 13b. The O_2 data from profile to profile are quite consistent, forming a tight temperature-O_2 relation. At temperatures in excess of about 7 °C there is some profile-to-profile variability, indicative of seasonal variations over the 150 day observation period. At temperatures below about 5 °C, where there is little seasonal change in oxygen concentration, there is very little profile-to-profile change in the temperature-O_2 relation (no more than about 2 μmol/kg).

The South Pacific at these latitudes has previously been only sparsely explored. A comparison between the historical database and the float-derived O_2 estimates is not possible for the upper ocean. The seasonal cycle in the upper ocean is too strong, and the variability in the historical O_2 database is too large for meaningful comparisons to be made. Since dissolved oxygen has no seasonal cycle at the parking depth of the floats, however, it is possible to compare the float measurements of O_2 at 2000 m with the historical data (Figure 13a). The first measured O_2 value at 2000 m from each of the floats has been compared in Figure 16 to the value derived from the 2000 m O_2

climatology, based on shipboard measurements, at the float position (Figure 13a). The float-derived O_2 values at 2000 m are generally lower than the climatology, as was also the case with the HOT comparisons (Figures 6a and 6b). There are several possible explanations for these offsets. First, the O_2 climatology shown in Figure 13a could be incorrect, due either to faulty historical data, mapping errors, or real changes in the deep O_2 distribution in the S. Pacific in recent decades. Each of these potential causes seems unlikely, since the historical data used here are known to be of excellent quality and other, more recent shipboard measurements in this region show values consistent with climatology. The contouring scheme shown in Figure 13 results from objective analysis of the historical data using a 300 km Gaussian correlation function. A hand-contoured plot of the deep O_2 in the region is similar to Figure 13, suggesting that this cannot be the cause of the apparent difference in data from the differing methodologies.

It is possible that the discrepancies in Figure 16 reflect a problem with the initial calibration of the O_2 sensors at the factory. This would seem to be unlikely, since each sensor is calibrated in a temperature-controlled bath, where sensor-derived values are compared to samples pulled from the bath and then analyzed by the Winkler method. Finally, it is possible that the float O_2 sensors could age after leaving the SBE factory. One of the features of the SBE oxygen sensor is that they are always polarized with an internal battery. Since the chemical reaction employed in the Clark cell is operative in air as well as seawater, continuous sensor degradation is possible, although the sensors are in most cases deployed within a few months of being manufactured. Presently each

of these scenarios is being investigated in order to assess the cause of the initial O_2 offsets seen both at Hawaii and in the S. Pacific float data.

There is seasonal variability in dissolved O_2 along the upper portions of the section (Figure 17) that is substantially larger than the apparent sensor drift of ~5 μmol/kg/y. Throughout the period of November 2005 through March of 2006, the western S. Pacific had relatively high dissolved O_2 in the upper 200 m of the water column and lower values in the eastern S. Pacific. Below 200 m, there is evidence of low O_2 water in the eastern portion of the section. This signal intensifies through the austral summer as low oxygen water is transported poleward along the continental margin. The first profiles (in early November of 2005) were from late spring, and the dissolved O_2 in the upper 150 m reached very high values, in excess of 260 μmol/kg in the upper ocean. By mid-January 2006 (one month into austral summer), as the water warmed, O_2 was less soluble in near surface waters. The surface O_2 values decreased by 20-30 μmol/kg. Two months later, in mid-March 2006 (near the end of austral summer), the surface O_2 had decreased by an additional 20 μmol/kg over much of the South Pacific. It is anticipated that these instruments should continue to operate for three to four more years and, as long as they do not disperse far from their initial positions, it will be possible to monitor the variability in dissolved O_2 across the South Pacific using data from these profiling floats. This will provide unprecedented views of oxygen cycling on the scale of an ocean basin. It will also be possible to assess the performance limits that will characterize relatively large chemical sensor arrays.

3.3. The RiverNet System: Monitoring Nitrate Flux in Rivers

Human induced changes in the nitrogen cycle on land[18, 90, 91] are recorded in the nitrogen flux of rivers, which integrate the landscape processes in their drainage basins. Increased rates of anthropogenic fixed nitrogen production have caused a four- to five-fold increase in the fixed nitrogen flux in the Mississippi River basin and in watersheds around the Baltic Sea, but have had little effect in Northeast Canada or Hudson Bay watersheds. Nitrogen fluxes have increased 8 to 13 fold in the heavily populated regions of the Northeast United States and Northern Europe. If the release of reactive nitrogen (N_r) into the environment is proportional to human population growth,[91] then ~570 Tg N y^{-1} of N_r will be released by 2050. This is ~2 times the N_r released globally in 1850.[18, 91] These changes will be recorded by the N flux in rivers.

Most river monitoring programs rely on monthly or weekly samples,[92] which under-sample many water quality variations. For example, intensive 2-hour sampling over a 102 day period in the River Maine, Northern Ireland showed that the concentrations of soluble and particulate P and nitrate N were significantly related to short-term variations in flow.[93] Using log-load, log-flow relationships, the load errors for weekly sampling of the River Main, relative to the high frequency samples, ranged from -20% to +45% for fixed N and P loads.[91] These results suggest that monitoring at weekly or monthly intervals, which creates a bias towards low flow conditions, can produce large errors when estimating river nutrient loads. However, more intensive river sampling

programs cannot be easily sustained and in situ monitoring systems that make measurements in the water and transmit data daily or in real time are required.[84]

The RiverNet program was created in 1999 to continuously monitor water quality and nitrate flux in the Neuse River basin of North Carolina on the Atlantic Coastal plain. Nitrate concentrations and discharge measurements have been made for 5 years at 8 different stations by the RiverNet program (http://rivernet.ncsu.edu). During the 2001 to 2004 period, nitrate concentration measurements were made hourly with WS Envirotech NAS 2E nitrate analyzers.[16] The NAS 2E requires chemicals and standards that are prepared and maintained with sterile techniques to avoid loss of nitrate in standards. The NAS 2E can make ~720 unattended measurements with one chemical payload, so it must be serviced every three weeks for hourly interval measurements. Stage measurements were made every 15 minutes by a USGS gauge station or a YSI 9620 Sonde, and converted to discharge with standard rating curve techniques. Nitrate concentrations were interpolated to 15-minute intervals and combined with the discharge measurements to estimate flux. In 2004, Satlantic ISUS UV nitrate analyzers similar to those described by Johnson and Coletti[7] were deployed in the basin and used to make measurements synchronously with the stage measurements at 15-minute intervals. The UV nitrate analyzers are sensitive to sediment accumulations on the optics during high flow turbidity events. This problem was addressed by cleaning the optics with a high pressure water pump before UV measurements are made.

Five-year records of nitrate concentration and river flow are shown at a station below a large waste water treatment plant in the upper Basin (Figure 18a), and in the lower basin just above the Neuse River estuary (Figure 18b). Large variations in nitrate concentrations were observed throughout the 5-year records at each station in the Basin at all frequencies that were sampled. These concentration variations are found during high and low flow conditions and may bias flux estimates. To illustrate the potential bias of under-sampling the high-frequency nitrate concentration variations, daily grab sample results were compared to NAS-2E measurements at hourly intervals and ISUS nitrate concentration measurements at 15 minute intervals over a four day period at a station in the upper basin of the river (Figure 19). A 0.45 mg/l concentration spike is seen in the highest frequency data. The daily sample interval resolved only a 0.1 mg/l concentration change over this same period, while the hourly sample interval resolved a 0.25 mg/l concentration peak.

Improved monitoring technologies with higher temporal resolution are required to eliminate errors in our N flux estimates from watersheds, particularly in watersheds affected by waste treatment plant point sources. However, there is much that remains to be learned about N flux in watersheds. It may be that the nitrogen concentration variations or "noise" seen in high temporal resolution concentration records is actually a signal that can help identify the importance of different N sources on a watershed scale. Managing surface water quality will be crucial in the future as population growth increase sewage discharges into surface waters, and as groundwater resources are over

committed or contaminated. Accurate surface water quality monitoring will be essential to make policy decisions to meet our population's water resources needs in the future.

3.4. Land/Ocean Biogeochemical Observatory

The large nutrient loads carried by rivers are focused into the coastal ocean through estuaries.[5, 18] These regions are difficult to monitor with sufficient temporal resolution because the interactions of river flow, tidal oscillations and stratified water columns can produce rapid changes in concentration. An example of an operational estuarine observatory that is capable of providing the chemical measurements that address the coupling of nutrient inputs and ecosystem response at the appropriate spatial and temporal scale is the Land/Ocean Biogeochemical Observatory (LOBO) located in Elkhorn Slough, CA. The watershed is dominated by row crops and the climate allows two to three harvests per year. The observatory network consists of moorings deployed throughout the 11 km waterway that extends inland from the Monterey Bay coastline (Figure 20). Each mooring is equipped with physical and chemical sensors and a telemetry system for data transmission via a wireless network. Nitrate and oxygen are measured with optical sensors.[7, 35] Data from each instrument is collected hourly by a microprocessor-based mooring controller and transmitted by wireless radio to a computer at the Monterey Bay Aquarium Research Institute in Moss Landing, CA. Once the data is received, it is made available through the Internet at http://www.mbari.org/lobo.

The 2.5 year-long data set from the LOBO L01 mooring located approximately 1.5 km inland from Monterey Bay (Figure 20) reveals the relationship between nitrate, salinity and rainfall in the lower estuary (Figure 21). Nearly all of the rainfall comes during winter, and each of the three winters that have been monitored autonomously with the LOBO network are characterized by periods of high nitrate concentrations and low salinities. The maximum nitrate concentrations (> 400 µM) occur during or after rainfall events and can be more than an order of magnitude higher than typical surface marine waters (0-20 µM). During long periods with little or no rainfall (typically May through November) the nitrate concentrations are much lower than the winter values. The high nitrate concentrations and low salinities are produced by runoff from the watershed that flows through cultivated fields and strips fertilizers from the soil.

Surprisingly, brief periods of low salinity and high nitrate can also persist during summer (Figure 21 and 22). A mechanistic understanding of nitrate inputs was identified by examining data from across the chemical sensor network at short timescales. Data from the sensor network records high nitrate, low salinity water moving from the mouth of Elkhorn Slough towards the inland regions during the rising tide (Figure 23). High nitrate pulses first appear shortly after low tide at the L01 mooring near the mouth of the Slough. These pulses appear at the L04 mooring in mid-Slough later on the tide (Figure 23). They reach the L02 mooring at the head of the Slough at high tide. The two freshwater point source regions of Elkhorn Slough are Carneros Creek at the head of the waterway and the Old Salinas River near the Mouth (Figure 20). The data shown in Figure 23 demonstrates that the high nitrate pulses originate at the Old Salinas River in

the lower estuary and propagate landward, a result that is contrary to intuition. The salinity at the L03 mooring, close to the Old Salinas River, fluctuates between nearly fresh and nearly marine water over the daily tidal cycle during all seasons of the year. This results from the tidally driven flow of salty water from Monterey Bay flowing upstream to L03 at high tide, and freshwater from the Old Salinas River that flows past the mooring towards the ocean during low tide. During the dry season, the freshwater source is irrigation runoff from the intense agriculture in the Salinas Valley. In wet periods, the freshwater comes from precipitation that flows over and through the fields. This produces a high nitrate/low salinity source of water at L03 (Figure 22) that enters the mouth of Elkhorn Slough during low tides. This high nitrate/low salinity water is then carried inland by the rising tide. The nitrate loading in the source changes on a seasonal basis as the balance between irrigation water and precipitation changes.

The nutrients carried into Elkhorn Slough are linked to elevated rates of primary production, and this must influence the daily changes in oxygen concentration.[45] However, the diel variation in O_2 concentration may also be influenced by transport processes. Long-term observations with a sensor network are key to the deconvolution of the important frequencies that drive spatial and temporal variability of O_2. For example, O_2 concentrations in the main channel exhibit repeatable patterns in diel variability that fluctuate at the spring-neap tidal period of 14 days (Figure 24). The diel O_2 amplitudes are determined by how much contact the marsh lands have with the water, and how fast the water and its accumulated oxygen is flushed out of the system. Thus, variability in oxygen concentration reflects both the productivity and respiration rates in the upper

regions of the slough combined with timing and size of the tide. During the time period shown in Figure 24, the photoperiod occurs during high tide, so that the subsequent ebb tide has a high oxygen signal that is characteristic of high daytime productivity in the upper regions of the slough. At other times of the year the photoperiod has changed phase with the tide, and high tides occur during the night. This produces the opposite results in the patterns described above; the diel variability occurs with low O_2 concentrations at low tide, the gradient of O_2 is towards lower concentrations in the upper slough, and the spring-neap pattern in average oxygen values is representative of periods with high respiration rates.

4. Conclusions and Future Prospects

In this review, we have summarized the work that is being done to develop chemical sensor networks that can be used for sustained and autonomous observations within natural aquatic systems. There is now a set of chemical sensors that are clearly capable of operating in situ for long periods of time. These sensors have demonstrated remarkable performance under very strenuous conditions. They validate the feasibility of making accurate chemical measurements in difficult environments for long time periods with no human intervention. While the data returned by these sensors, in some cases, do not match the highest precisions and accuracies available with laboratory measurements, the continuous data records that they return can provide a much broader perspective on environmental processes. The situation is, in some regards, similar to measurement of ocean chlorophyll concentrations using satellite-borne ocean color sensors. The satellite

measurements at any one surface location are not nearly as precise or accurate as laboratory based measurements of chlorophyll.[94] However, the global picture returned by satellites is much richer and reveals processes that could not be detected by ship-board sample collection. In this same sense, the data that have been returned with autonomous chemical sensor systems have provided an unprecedented view of biogeochemical cycling that could not be obtained with conventional sampling. It is clearly possible to consider the operation of global-scale chemical sensor networks.

The technologies that enable long-term, autonomous observations will be expanded to additional chemicals. A particularly vital need exists for pH or other carbon system sensors that can compliment the existing pCO_2 sensors and which can be used for profiling to ocean depths. In situ sensors also demonstrate the role that chemical speciation plays in determining bioavailability of ecologically important chemicals.[33] Measurements of chemical speciation have not yet been made in situ for long time periods, but there is a critical need to develop this capability. Long-term, in situ measurements of trace elements such as iron are also critical for our understanding of the role that they play in structuring aquatic ecosystems. Efforts to develop in situ analyzers that are capable of detecting trace elements at sub-nanomolar concentrations, which are typical of the marine environment,[2] are just beginning.[95]

Existing sensors can also be adapted to additional platforms. For example, it appears to be straightforward to modify optical nitrate sensors presently employed in moored applications for use on profiling floats.[7] In combination with oxygen, this would

allow observations of the processes that drive primary production (nutrient availability) and the ecosystem response (oxygen production and consumption). However, it is also clear that most chemical species will still have to be analyzed in samples that are returned to the laboratory. The rate of progress in developing new sensors capable of long-term operation is not rapid enough to anticipate the time when a much broader suite of chemicals can be sensed autonomously. One of the significant roles of a long-term chemical sensor network will be to provide the contextual information on variations in major biogeochemical processes within which more focused environmental studies can be made using more complex instrumentation.

5. Acknowledgments

Work at MBARI was supported by the National Science Foundation through the Biocomplexity in the Environment Program Grant ECS-0308070 and by a grant from the David and Lucile Packard Foundation. Research at the University of Washington was supported by National Oceanic and Atmospheric Administration Grant NA17RJ1232 Task 2 and by Office of Naval Research contract ONR NOOO14-03-1-0446. Research at North Carolina State University was supported by National Science Foundation Grant GEO-0303195 and by the North Carolina Department of Environment and Natural Resources.

6. References

(1) Emery, W. J.; Thomson, R. E. *Data analysis methods in physical oceanography, 2nd Ed.*, Elsevier: Amsterdam, Holland, 2001; 638 pp.

(2) Johnson, K. S.; Coale, K. H.; Jannasch, H. W. *Anal. Chem.* **1992**, *64*, 1065A.

(3) de Jonge, V. N.; Elliott, M.; Brauer, V. S. *Mar. Pollut. Bull.* **2006**, *53*, 5.

(4) Magnuson, J. J. *BioScience* **1990**, *40*, 495.

(5) National Research Council, *Clean coastal waters: understanding and reducing the effects of nutrient pollution*, National Academy Press: Washington, DC, **2000**; 405 pp.

(6) Johnson, K. S.; Coletti, L. J.; Chavez, F. P. *Deep-Sea Res. I* **2006**, *53*, 561.

(7) Johnson, K. S.; Coletti, L. J. *Deep-Sea Res. I* **2002**

(8) Bell, J.; Betts, J.; Boyle, E. *Deep-Sea Res. I* **2002**, *49*, 2103.

(9) Jannasch, H. W.; Wheat, C. G.; Plant, J. N.; Kastner, M.; Stakes, D. S. *Limnol. Oceanogr.: Methods* **2004**, *2*, 102.

(10) Wallace, D. W. R.; Wirick, C. D. *Nature* **1992**, *356*, 694.

(11) McGillicuddy D. J. Jr.; Robinson, A. R.; Siegel, D. A.; Jannasch, H. W.; Johnson, R.; Dickey, T. D.; McNeil, J.; Michaels, A. F.; Knapp, A. H. *Nature* **1998**, *394*, 263.

(12) McNeil, J. D.; Jannasch, H. W.; Dickey, T.; McGillicuddy, D.; Brzezinski, M.; Sakamoto, C. M. *J. Geophys. Res.* **1999**, *104*, 15,537.

(13) Chavez F. P.; Strutton, P. G.; Friederich, G. E.; Feely, R. A.; Feldman, G. C.; Foley, D. G.; McPhaden, M. J. *Science* **1999**, *286*, 2126.

(14) Friederich, G. E.; Walz, P. M.; Burczynski, M. G.; Chavez, F. P. *Progr. Oceanogr.* **2002**, *54*, 185.

(15) Sakamoto, C. M.; Karl, D. M.; Jannasch, H. W.; Bidigare, R. R.; Letelier, R. M.; Walz, P. M.; Ryan, J. P.; Polito, P. S.; Johnson, K. S. *J. Geophys. Res.* **2004**, *109*, C05032, doi:10.1029/2003JC001976.

(16) Hydes, D. J.; Wright, P. N.; Rawlinson, M. B. In *Chemical sensors in oceanography*, Varney, M. S., Ed.; Gordon and Breach: Amsterdam, The Netherlands, **2000**; pp 95-105.

(17) Baehr, M. M.; DeGrandpre, M. D. *Limnol. Oceanogr.* **2004**, *49*, 330.

(18) Vitousek, P. M.; Aber, J. D.; Howarth, R. W.; Likens, G. E.; Matson, P. A.; Schindler, D. W.; Schlesinger, W. H.; Tilman, D. G. *Ecol. Appl.* **1997**, *7*, 737.

(19) Rojstaczer, S.; Sterling, S. M.; Moore, N. J. *Science* **2001**, *294*, 2450.

(20) Jackson, R. B.; Carpenter, S. R.; Dahm, C. N.; McKnight, D. M.; Naiman, R. J.; Postel, S. L.; Running, S. W. *Ecol. Appl.* **2001**, *11*, 1027.

(21) Battle, M.; Bender, M. L.; Tans, P. P.; White, J. W. C.; Ellis, J. T.; Conway, T.; Francey, R. J. *Science* **2000**, *287*, 2467.

(22) Keeling, R. F.; Shertz, S. R. *Nature* **1992**, *358*, 723.

(23) Roemmich, D.; Riser, S.; Davis, R.; Desaubies, Y. *Mar. Technol. Soc. J.* **2004**, *38*, 31.

(24) Lewis, E. L. *IEEE J. Oceanogr. Eng.* **1980,** *5*, 3.

(25) Schlitzer, R. *EOS Trans. Am. Geophys. Union* **2000**, *81*, 45.

(26) Kortzinger, A.; Shimanski, J.; Send, U.; Wallace, D. *Science* **2004**, *306*, 1337.

(27) Buffle, J.; Horvai, G. Eds. *In situ monitoring of aquatic systems; Chemical analysis and speciation*, Vol. 6, IUPAC Series on Analytical and Physical Chemistry of Environmental Systems: Wiley: Chichester, England, 2000; 623 pp.

(28) Varney, M. Ed. *Chemical sensors in oceanography*: Gordon and Breach: Amsterdam, The Netherlands, 2000, 333 pp.

(29) Taillefert, M.; Luther, G. W.; Nuzzio, D. B. *Electroanalysis* **2000**, *12*, 401.

(30) Daly, K. L.; Byrne, R. H.; Dickson, A. G.; Gallagher, S. M.; Perry, M. J.; Tivey, M. K. *Mar. Tech. Soc. J.* **2004**, *38*, 121.

(31) Volpe, A. M.; Esser, B. K.; Bianchini, G. M. *J. Anal. At. Spectrom.* **2001**, *16*, 801.

(32) Clark, L. C. Trans. Am. Soc. Artif. Intern. Organs **1956**, 2, 41.

(33) Luther, III, G. W.; Rozan, T. F.; Taillefert, M.; Nuzzio, D. B.; Di Meo, C.; Shank, T. M.; Lutz, R. A.; Cary, S. C. *Nature* **2001**, *410*, 813.

(34) Glud, R. N.; Klimant, I.; Holst, G.; Kohls, O.; Meyer, V.; Kuehl, M.; Gundersen, J. K. *Deep-Sea Res. I* **1999**, *46*, 171.

(35) Tengberg, A.; Hovdenes, J.; Andersson, H. J.; Brocandel, O.; Diaz, R.; Hebert, D.; Arnerich, T.; Huber, C.; Kortzinger, A.; Khripounoff, A.; Rey, F.; Ronning, C.; Schimanski, J.; Sommer, S.; Stangelmayer, A. *Limnol. Oceanogr. Methods* **2006**, *4*, 7.

(36) Clayson, C. H. In *Chemical sensors in oceanography*, Varney, M. S., Ed.; Gordon and Breach: Amsterdam, The Netherlands, 2000; pp 107-121.

(37) DeGrandpre, M. D.; Baehr, M. M. *Anal. Chem.* **1999**, *71*, 1152.

(38) Chavez, F.P.; Wright, D.; Herlien, R.; Kelley, M.; Shane, F.; Strutton, P.G. J. Atmos. Ocean. Technol. **2000,** 17, 215.

(39) Manov, D. V.; Chang, G. C.; Dickey, T. D. *J. Atm. Ocean. Technol.* **2004**, *21*, 958.

(40) Ruzicka, J.; Hansen, E. H., *Flow Injection Analysis, 2nd ed.*; Wiley: New York, 1985, 498.

(41) Blain, S.; Jannasch, H. W.; Johnson, K. S. In *Chemical sensors in oceanography*, Varney, M. S., Ed.; Gordon and Breach: Amsterdam, The Netherlands, 2000; pp 49-70.

(42) Johnson, K. S.; Elrod, V. A.; Nowicki, J. L.; Coale, K. H.; Zamzow, H. In *In situ monitoring of aquatic systems; Chemical analysis and speciation*, Buffle, J.; Horvai, G. Eds.; IUPAC Series on Analytical and Physical Chemistry of Environmental Systems, Vol. 6: Wiley: Chichester, England, 2000; pp 223-252.

(43) Odum, H. T. *Limnol. Oceanogr.* 1956, *1*, 103.

(44) Rablais, N. N. *Ambio* **2002**, *31*, 102.

(45) Caffrey, J. M. *Env. Monit. Asses.* **2003**, *81*, 207.

(46) Emerson, S; Stump, C; Johnson, B; Karl, DM *Deep-Sea Res. I* **2002**, *49*, 941.

(47) Beck, N. G.; Fisher, A. T.; Bruland, K. W. *Mar. Ecol. Progr. Ser.* **2001**, *217*, 43.

(48) Rudnick, D. L.; Davis, R. E.; Eriksen, C. C.; Fratantoni, D. M.; Perry, M. J. *Mar. Technol. Soc. J.* **2005**, *38*, 48.

(49) Karl, D. M.; Lucas, R. *Deep-Sea Res. Part II* **1996**, *43*, 129.

(50) Grasshoff K. (1983) In: *Methods of Seawater Analysis, 2nd edition*. Grasshoff, K.; Ehrhardt, M.; Kremling, K. Eds.; Verlag Chemie: New York, 1983; pp .

(51) Demas J. N.; DeGraff, B. A.; Coleman, P. B. *Anal. Chem.* **1999**, *71*, 793A.

(52) Kortzinger, A.; Schimanski, J.; Send, U. *J. Atm. Ocean. Technol.* **2005**, *22*, 302.

(53) Glazer, B. T.; March, A. G.; Stierhoff, K.; Luther, G. W. *Anal. Chim. Acta* **2004**, *518*, 93.

(54) Atkinson, M. J. *Limnol. Oceanogr.* **1988**, *33*, 141.

(55) Berg, P.; Roy, H.; Janssen, F.; Meyer, V.; Jorgensen, B. B.; Huettel, M.; de Beer, D. *Mar. Ecol. Prog. Ser.* **2003**, *261*, 75.

(56) McNeil, C.L.; Johnson, B.D.; Farmer, D.M. *Deep-Sea Res. I* **1995**, *42*, 819.

(57) Kennett, J. P.; Cannariato, K. G.; Hendy, I. L.; Behl, R. J. *Science* **2000**, *288*, 128.

(58) Kim, G.; Hwang, D.-W. *Geophys. Res. Lett.* **2002**, *29*, 1678, 10.1029/2002GL015093.

(59) DeGrandpre, M. D.; Hammar, T. R.; Wallace, D. W. R.; Wirick, C .D. *Limnol. Oceanogr.* **1997**, *42*, 21.

(60) Hood, E. M.; Merlivat, L. *J. Mar. Res.* **2001**, *59*, 113.

(61) DeGrandpre, M. D.; Hammar, T. R.; Smiith, S. P.; Sayles, F. L. *Limnol. Oceanogr.* **1995**, *40*, 969.

(62) Lefevre, N.; Ciabrini, J. P.; Michard, G.; Brient, B.; DuChaffaut, M.; Merlivat, L. *Mar. Chem.* **1993**, *42*, 189.

(63) Friederich, G. E.; Brewer, P.G.; Herlein, R.; Chavez, F. P. *Deep-Sea Res. I* **1995**, *42*, 1175.

(64) Hanson, P. C.; Bade, D. L.; Carpenter, S. R.; Kratz, T. K. *Limnol. Oceanogr.* **2003**, *48*, 1112.

(65) Byrne, R. H.; McElligott, S.; Feely, R. A.; Millero, F. J. *Deep-Sea Res. I* **1999**, *46*, 1985.

(66) Martz, T. R.; Carr, J. J.; French, C. R.; DeGrandpre, M. D. *Anal. Chem.* **2003**, *75*, 1844.

(67) Watanabe, A.; Kayanne, H.; Nozaki, K.; Kato, K.; Negishi, A.; Kudo, S.; Kimoto, H.; Tsuda, M.; Dickson, A. G. *Mar. Chem.* **2004**, *85*, 75.

(68) Grasshoff, K.; Kremling, K.; Erhardt, M. Eds. *Methods of Seawater Analysis*, Wiley: Chichester, England, 1999; 447 pp.

(69) Jannasch, H. W.; Johnson, K. S.; Sakamoto, C. M. *Anal. Chem.* **1994**, *66*, 3352.

(70) Chapin, T. P.; Caffrey, J. M., Jannasch, H. W.; Coletti, L. J.; Haskins, J. C.; Johnson, K. S. *Estuaries* **2004**, *27*, 882.

(71) Thouron, D.; Vuillemin, R.; Philippon, X.; Lourenco, A.; Provost, C.; Cruzado, A.; Garcon, V. *Anal. Chem.* **2003**, *75*, 2601.

(72) Chapin, T. P.; Jannasch, H. W.; Johnson, K. S. *Anal. Chim. Acta* **2002**, *463*, 265.

(73) Sharples, J.; Moore, C. M.; Abraham, E. R. *J. Geophys. Res.* **2001**, *106*, 14,069.

(74) Sigleo, A.C.; Mordy, C. W.; Stabeno, P.; Frick, W. E. *Est. Coastal Shelf Sci.* **2005**, *64*, 211.

(75) Weston, K.; Jickells, T. D.; Fernand, L.; Parker, E. R. *Est. Coastal Shelf Sci.* **2004**, *59*, 559.

(76) Muller, B.; Reinhardt, M.; Gachter, R. *J. Environ. Monit.* **2003**, *5*, 808.

(77) Le Goff, T.; Braven, J.; Ebdon, L.; Scholefield, D. *J. Environ. Monit.* **2003**, *5*, 353.

(78) Scholefield, D.; Le Goff, T.; Braven, J.; Ebdon, L.; Long, T.; Butler, M. *Sci. Total Environ.* **2005**, *344*, 201.

(79) Pressl, A.; Winkler, S.; Gruber, G. *Water Sci. Technol.* **2004**, *50*, 67.

(80) Bishop, J. K. B.; Calvert, S. E.; Soon, M. Y. S. *Deep-Sea Res. II* **1999**, *46*, 2699.

(81) Bishop, J.K.B.; Davis, R.E.; Sherman, J.T. *Science* **2002**, *298*, 817.

(82) Bishop, J. K. B.; Wood, T. J.; Davis, R. E.; Sherman, J. T. *Science* **2004**, *304*, 417.

(83) Porter, J.; Arzberger, P.; Braun, H.-W.; Bryant, P.; Gage, S.; Hansen, T.; Hanson, P.; Lin, C.-C.; Lin, F.-P.; Kratz, T.; Michener, W.; Shapiro, S.; Williams, T. *Bioscience* **2005**, *55*, 561.

(84) Glasgow, H. B.; Burkholder, J. M.; Reed, R. E.; Lewitus, A. J.; Kleinman, J. E. *J. Exp. Mar. Biol. Ecol.* **2004**, *300*, 409.

(85) Effler, S. W.; O'Donnell, D. M.; Owen, C. J. *J. Urban Technol.* **2002**, *9*, 21.

(86) Vivoni, E. R.; Camilli, R. *Comput. Geosci.* **2003**, *29*, 457.

(87) Wenner, E. L.; Geist, M. *Coastal Management* **2001**, *29*, 1.

(88) Tedesco, M.; Bohlen, W. F.; Howard-Strobel, M. M.; Cohen, D. R.; Tebeau, P. A. *Environ. Monit. Asses.* **2003**, *81*, 35.

(89) Grasshoff, K. In *Marine Electrochemistry*, Whitfield, M.; Jagner, D., Eds.; John Wiley: Chichester, England, 1981; pp 327-420.

(90) Howarth, R. W. *Water Sci. Technol.* **2004**, *49*, 7.

(91) Galloway, J. N.; Dentener, F. J.; Capone, D. G.; Boyer, E. W.; Howarth, R. W.; Seitzinger, S. P.; Asner, G. P.; Cleveland, C. C.; Green, P. A.; Holland, E. A.; Karl, D. M.; Michaels, A. F.; Porter, J. H.; Townsend, A. R.; Vorosmarty, C. J. *Biogeochemistry* **, 2004**, *70*, 153.

(92) Zhang, Y. K.; Schilling, K. *Adv. Water Resour.* **2005,** *28*, 701.

(93) Stevens, R. J.; Smith, R. V. *Water Res.* **1978**, *12*, 823.

(94) Hooker, S. B.; McClain, C. R. *Progr. Oceanogr.* **2000**, *45*, 427.

(95) Laes, A.; Vuillemin, R.; Leilde, B.; Sarthou, G.; Bournot-Marec, C.; Blain, S. *Mar. Chem.* **2005**, *97*, 347.

Figure Legends

Figure 1. Measurements of temperature, nitrate and chlorophyll made at hourly intervals for one year on the M1 mooring 20 km offshore in Monterey Bay, California. Nitrate was measured with a nitrate sensor.[7] Chlorophyll concentration was calculated from the attenuation of sunlight at 490 nm between the surface and 10 m. Measurements of nitrate and chlorophyll in samples collected near the mooring at approximately 21 day intervals are shown as open circles. Adapted from Johnson et al.[6]

Figure 2. Salinity measured on the Practical Salinity Scale[24] at 200 m depth in the Pacific Ocean. The map was contoured using the program OceanDataView[25] after importing vertical profile data for ~1200 Argo floats from the Argo data center (ftp://ftp.ifremer.fr/ifremer/coriolis/global_profile/pacific_ocean/). Data was collected during the first 2 weeks of Dec. 2005. The location of each vertical profile is shown as a black dot.

Figure 3. An ISUS optical nitrate sensor encrusted with hydroids. Red arrows identify the outside diameter of the instrument (12.5 cm) and the green arrow points to a copper anti-fouling sheild that protects the optics.

Figure 4. The trajectory of UW float 0894 near the Hawaiian Islands, deployed in August of 2002. The red dots show the location of the profiles at 10-day intervals. The

green dot denotes the location of profile 009, shown in Figure 5. This float was parked at a depth of 1000 m and collected data from 2000 m on every fourth profile.

Figure 5. Temperature, salinity, and dissolved O2 profiles from UW float 0894, profile 009. The dots denote the pressures where data were collected. The position where these data were collected is denoted by the green dot along the trajectory of Float 0894 shown in Figure 4.

Figure 6. A) Time series of shipboard surface O2 data collected at the HOT site, near 22 °N, 158 °W (red dots), and O2 data from a depth of 5 m collected by float 0894 (blue dots). B) Time series of shipboard 2000 m O2 data collected at the HOT site, near 22 °N, 158 °W (green dots), and O2 data from a depth of 2000 m collected by float 0894 (red dots). The shipboard values were determined using the Winkler titration method.

Figure 7. Oxygen concentration measured over 580 days at 1800 m depth on an Argo profiling float in the Labrador Sea. Density values calcuated from temperature, salinity and pressure are also shown. The average oxygen concentration was 295.0±0.7 (1 SD) µmol/L for the 580 day period. The shift in density and oxygen at ~360 days suggests that some of the concentration variability occurred as the float entered a new water mass with different properties. Reproduced from Tengberg et al.[35] with permission.

Figure 8. A 3.5 month time series of pCO2 (top) and dissolved oxygen concentration (bottom) in Placid Lake, Montana during the transition from the lake covered with ice, through melting and into the spring bloom. Measurements were made with instruments at 2m (black lines) and 20 m (dotted lines). Atmospheric equilibrium values are shown as dotted lines marked atm. The two vertical dash-dotted lines bracket the three distinct physical periods discussed in the text: (1) under-ice near isothermal conditions (19 March–23 April), (2) post–ice-out deep mixing (23 April–18 May), and (3) stable stratification (18 May–2 July). From Baehr and Degrandpre[17] with permission.

Figure 9. Measurements of (A) seasurface height anomaly (note inverted scale), (B) temperature at 180 m (note inverted scale), (C) daily average nitrate concentration at 180 m, and (D) daily average chlorophyll concentration at 25 m on the HALE/ALOHA mooring at the Hawaii Ocean Timeseries station north of Oahu. Seasurface height anomaly was measured by the Topex/Poseidon satellite altimeter. Nitrate was measured with an osmotically powered chemical analyzer.[69] Nitrate concentrations measured in samples collected near the mooring during HOT program monthly visits by ship are show as black circles. Chlorophyll was determined from the attenuation of sunlight at 490 nm. Adapted from Sakamoto et al.[15]

Figure 10. A) Nitrate concentration measured on the M1 mooring 20 km offshore in Monterey Bay, CA using an optical nitrate sensor during 5 days in 2004. B) Nitrate concentrations after high-pass filtering the data to remove frequencies lower than 0.7 cycles/d. The decrease in high-pass filtered nitrate concentration during daylight is

presumed to be due to biological uptake at a fixed ratio to carbon of 16 N/106 C, typical of phytoplankton. C) Photosynthetically active radiation measured on the mooring with a spectral radiometer. D) Monthly average values of primary production, which were calculated from daily uptake of nitrate concentrations measured by autonomous sensors on the M1 mooring as shown in (B) and a N/C ratio of 16/106 are shown for 3 years from 1/2002 to 12/2004 (open triangles). The upwelling index (m^3 water upwelled/100 m coastline/s), calculated from wind speed and direction and coastline orientation is also shown for Monterey Bay (solid circles). Adapted from Johnson et al.[6]

Figure 11. Measurements of the sea-air difference in CO_2 partial pressure made on a mooring in Monterey Bay using autonomous sensor technology. The impact of 1997 El Niño/La Niña on the carbon dioxide system is manifested by low variability in 1997/1998 due to weakened upwelling. Reproduced from Friederich et al.[14] with permission.

Figure 12. Locations (solid circles) where measurements of pCO_2 are made on remote moorings by the MBARI/NOAA sensor network. Data from these moorings can be accessed on the Internet at http://www.pmel.noaa.gov/co2/moorings/.

Figure 13. A) Dissolved O2 (mmol/kg) at a depth of 2000 m in the South Pacific (red contours), determined by objectively analyzing historical data for the region using a Gaussian 300 km correlation function. The historical station data used in the calculation (positions noted by the green dots) were determined using the Winkler titration method.

Deployment locations of 22 profiling floats with dissolved O2 sensors are shown by the blue dots. The trajectories of the floats from November 2005 through March 2006 are shown as the black lines emanating from the blue dots. B) The trajectory of UW float 2348 from the S. Pacific, deployed in November of 2005. The figure shows the location of the float through March of 2006. The red dots denote profile locations. The float was parked at a depth of 2000 m.

Figure 14. The 2000 m dissolved O2 climatology at the position of the first float profile (see Figure 4 for float deployment locations) plotted against the float-derived 2000 m O2 value for the first profile, for each of the 22 floats shown in Figure 13. The line shows the least-squares fit between the float O2 and the climatology.

Figure 15. A diagram showing the temperature-dissolved O2 relation for the first 18 profiles of float 2348 (see Figure 13 for the locations of these profiles). Note the lack of scatter in the data below about 7 °C, indicating the lack of sensor drift.

Figure 16. The change in dissolved O2 compared to climatology at 2000 m relative to the value measured at 2000 m on profile 001, for each of the 22 floats deployed in the S. Pacific (see Figure 13). Note that 20 of the 22 instruments showed a weak drift over time towards lower values, while two of the instruments showed a much larger drift. The large drift is presumed to be due to faulty sensors and data from these two instruments has not been used.

Figure 17. Sections of dissolved O2 in the upper 400 m across the S. Pacific, determined from 20 profiling floats deployed in November of 2005. Data from two of the floats (2340 and 5025) have not been used in this calculation due to the extreme drift exhibited by these two sensors. The positions of the floats are shown in Figure 13. The positions of the float profiles along the sections are noted by the dotted lines.

Figure 18. A 5 year time series of nitrate concentration measured with in situ sensors (green line), nitrate measured in discrete samples (red diamonds) and river stage (black line) in the upper Neuse River basin just below a waste water treatment plant (A), and in the lower Neuse River Basin just above the Neuse River Estuary (B).

Figure 19. Comparison of grab samples (red circles), hourly measurements in situ with a NAS-2E analyzer (open diamonds), and 15 minute nitrate measurements with an ISUS optical nitrate sensor (black circles) during a nitrate concentration spike in the upper Neuse River basin.

Figure 20. Map of Elkhorn Slough, CA showing the location of the moorings that house the sensors for the Land/Ocean Biogeochemical Observatory. Data from each mooring is accessible at http://www.mbari.org/lobo.

Figure 21. Salinity (A), Nitrate (B), at the L01 mooring of the Land/Ocean Biogeochemical sensor network measured from November 2003 to April 2006. Also

shown is daily precipitation (C) at a nearby weather station. Nitrate was measured with an optical nitrate sensor.[7]

Figure 22. Nitrate-Salinity relationship at the mooring L03 for the periods March 2005 (filled circles), August 2005 (open circles) and December 2005 (open triangles).

Figure 23. Nitrate and salinity, over a four day period at three locations in Elkhorn Slough, CA. A) L01 – 1.0 km inland (from Highway 1 bridge), B) L04 – 4.0 km inland, and C) L02 – 6.9 km inland. The solid green line indicates the relative tide height.

Figure 24. Oxygen at three locations in Elkhorn Slough, CA. A) L01 – 1 km inland (from Monterey Bay), B) L04 – 3 km inland, and C) L02 – 8 km inland. Also shown is the tidal cycle (D).

Figure 9

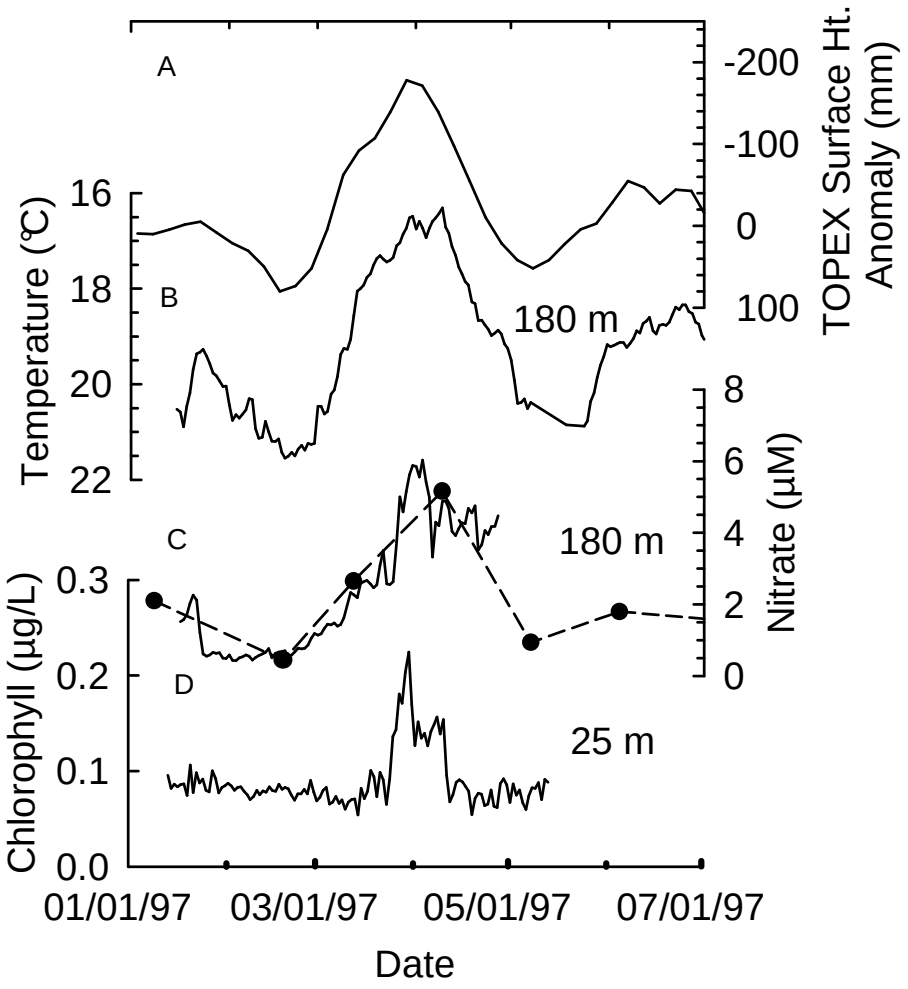
A
B
C
D
180 m
180 m
25 m
Temperature (℃)
16
18
20
22
TOPEX Surface Ht. Anomaly (mm)
-200
-100
0
100
Nitrate (µM)
8
6
4
2
0
Chlorophyll (µg/L)
0.3
0.2
0.1
0.0
01/01/97
03/01/97
05/01/97
07/01/97
Date

Figure 10

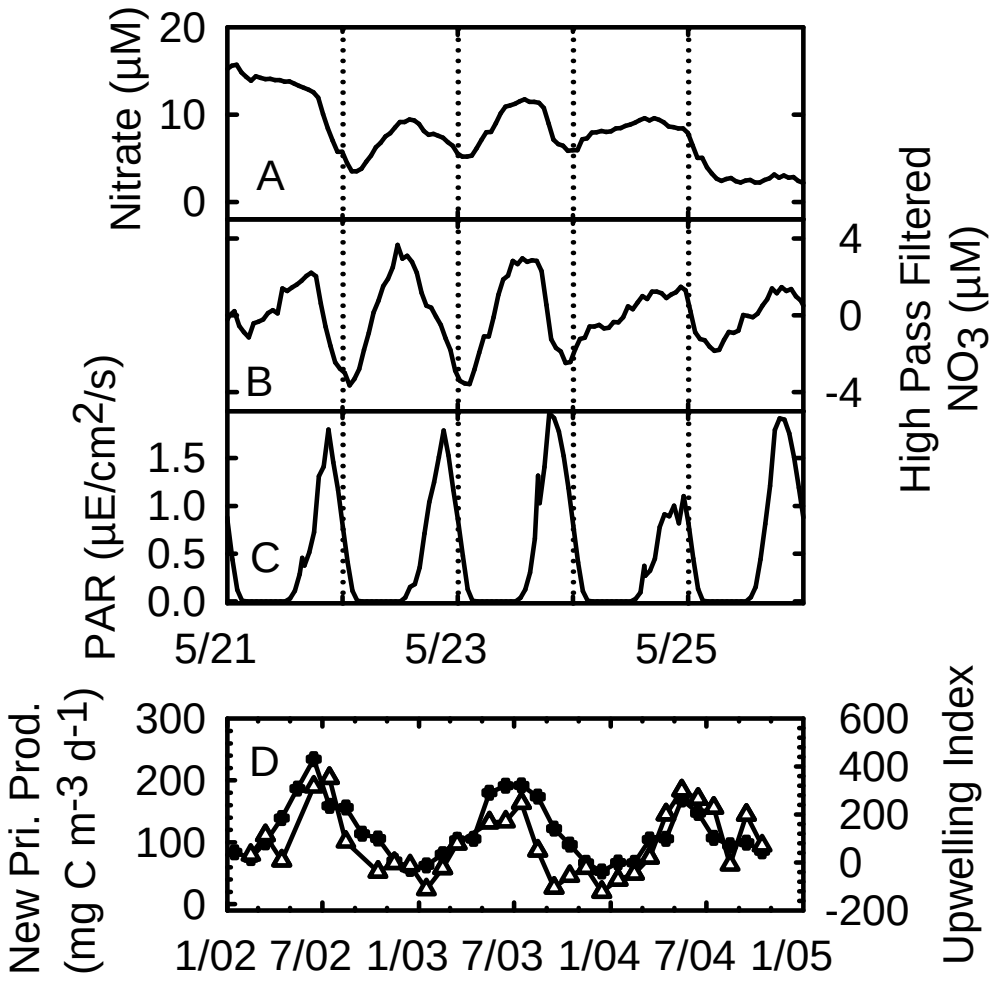
Nitrate (µM)
20
10
0
A
B
C
4
0
-4
High Pass Filtered
NO3 (µM)
PAR (µE/cm2/s)
1.5
1.0
0.5
0.0
5/21
5/23
5/25
New Pri. Prod.
(mg C m-3 d-1)
300
200
100
0
D
600
400
200
0
-200
Upwelling Index
1/02 7/02 1/03 7/03 1/04 7/04 1/05

Figure 11

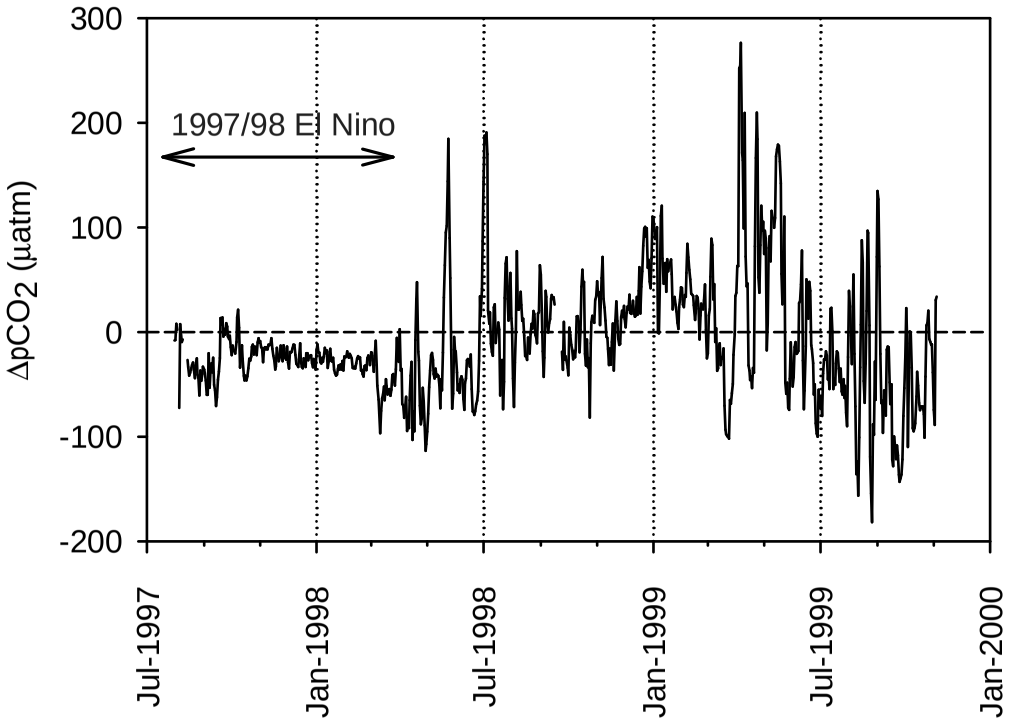
300
200
100
0
-100
-200
ΔpCO2 (µatm)
1997/98 El Nino
Jul-1997
Jan-1998
Jul-1998
Jan-1999
Jul-1999
Jan-2000

Figure 12

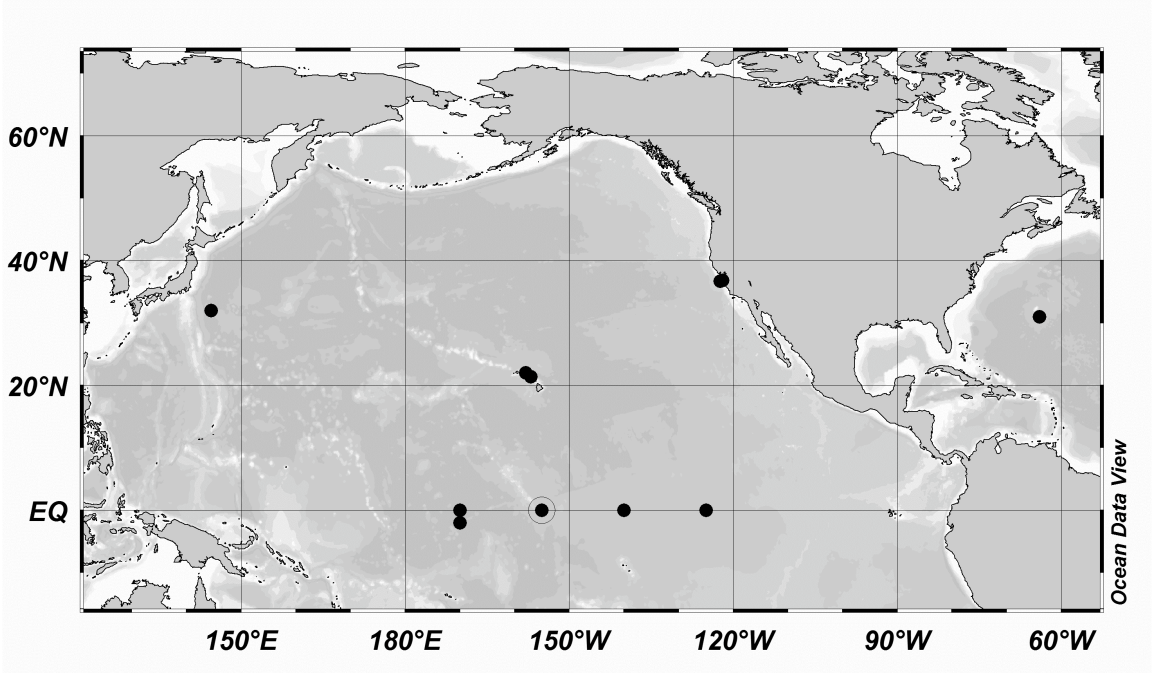

Figure 13

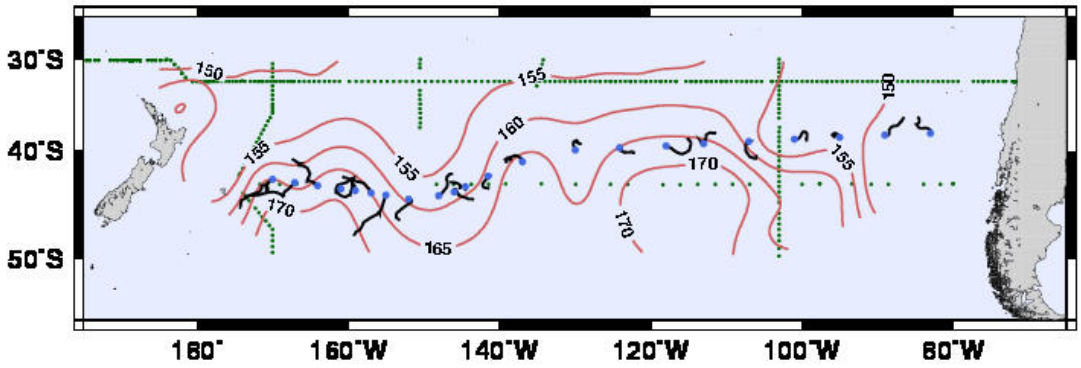
30°S
40°S
50°S
160°
160°W
140°W
120°W
100°W
80°W
150
155
160
165
170
155
150
155
170
165
170

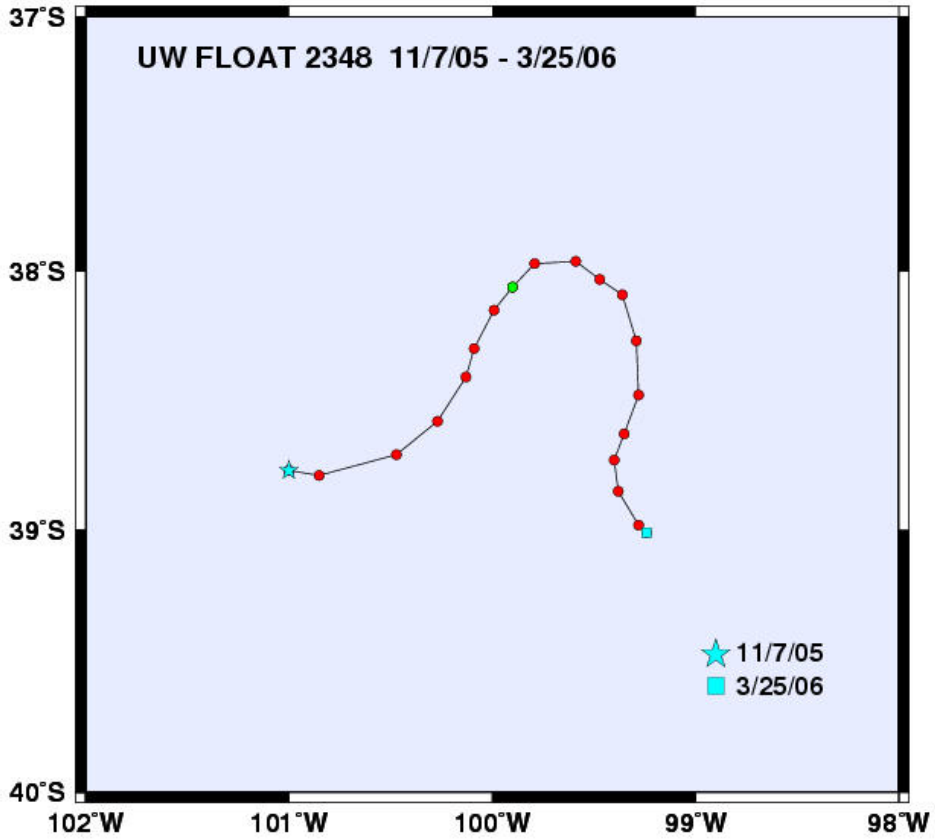
UW FLOAT 2348 11/7/05 - 3/25/06
37°S
38°S
39°S
40°S
102°W
101°W
100°W
99°W
98°W
11/7/05
3/25/06

Figure 14

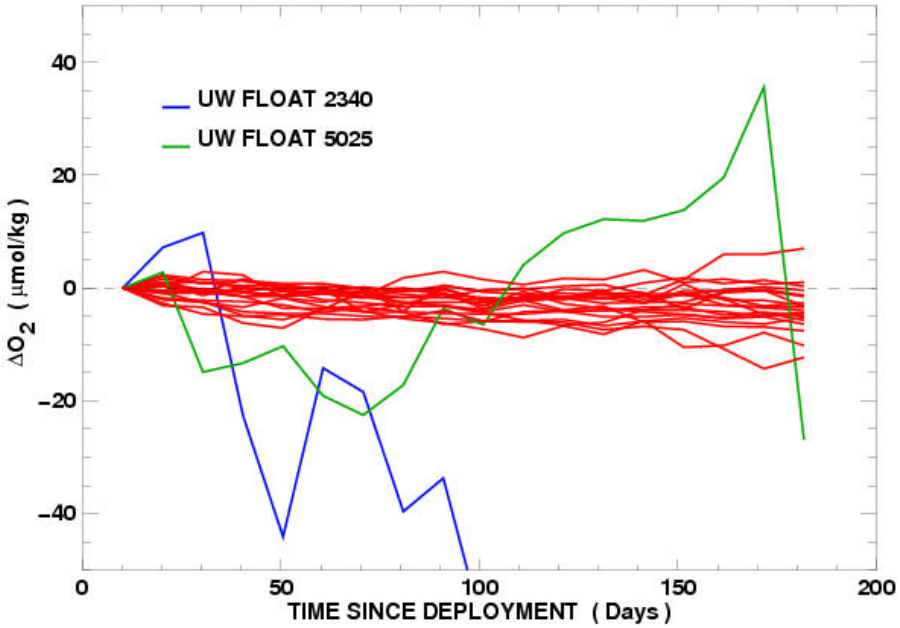
UW FLOAT 2340
UW FLOAT 5025
40
20
0
−20
−40
ΔO2 (μmol/kg)
0
50
100
150
200
TIME SINCE DEPLOYMENT (Days)

Figure 15

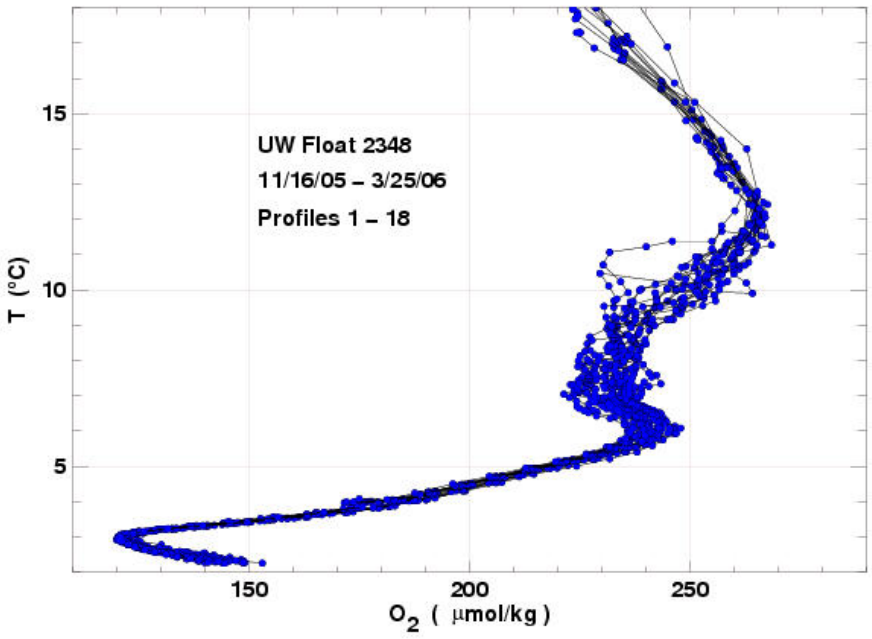
UW Float 2348
11/16/05 – 3/25/06
Profiles 1 – 18
T (°C)
15
10
5
150
200
250
O2 (µmol/kg)

Figure 16

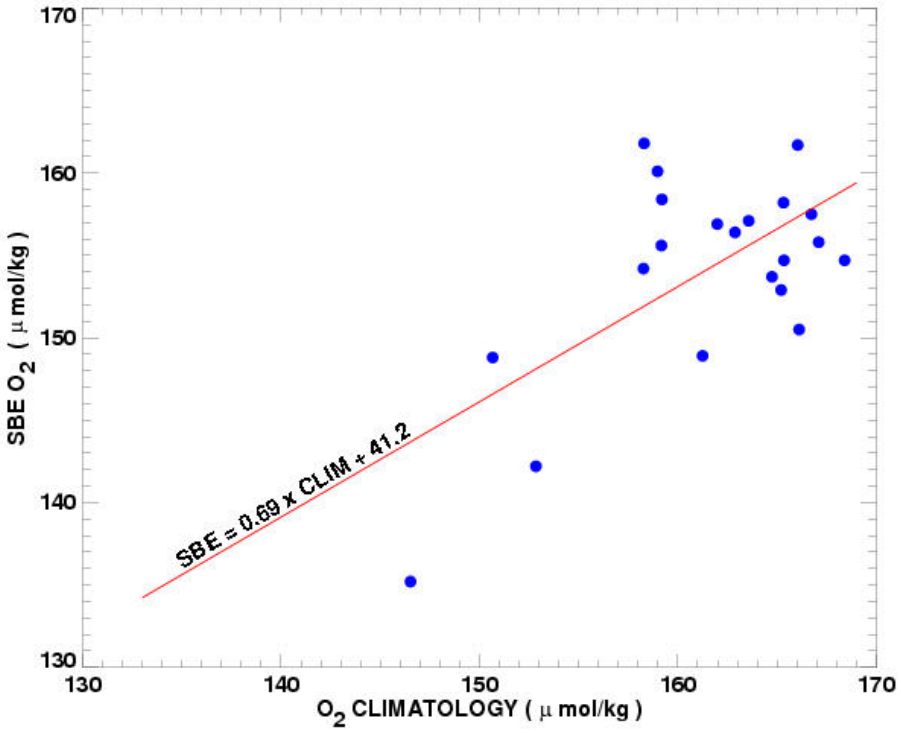
170
160
150
140
130
130
140
150
160
170
SBE O2 (μ mol/kg)
O2 CLIMATOLOGY (μ mol/kg)
SBE = 0.69 x CLIM + 41.2

Figure 17

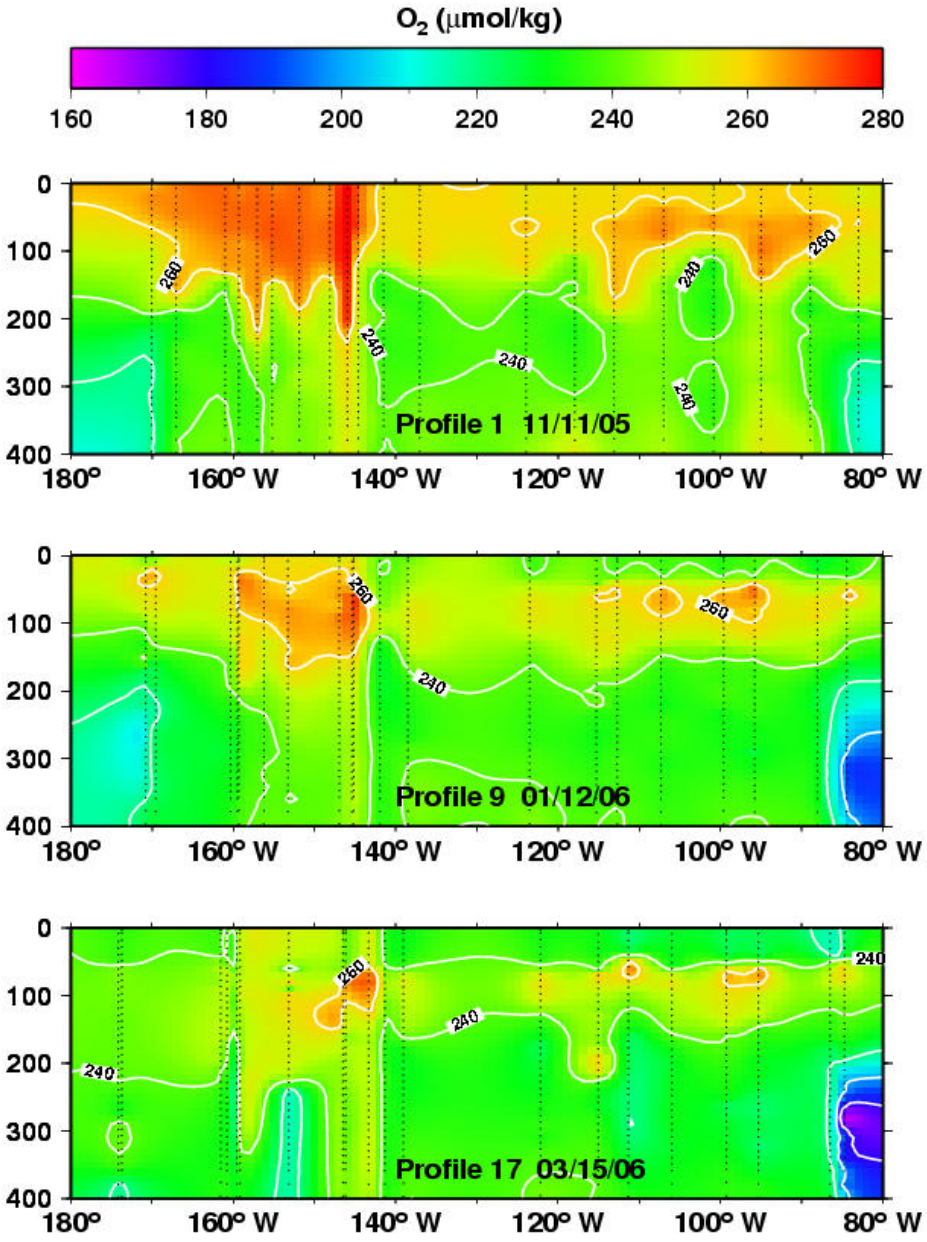
O2 (μmol/kg)
160
180
200
220
240
260
280
0
100
200
300
400
260
240
240
240
260
240
Profile 1 11/11/05
180°
160° W
140° W
120° W
100° W
80° W
0
100
200
300
400
260
260
240
Profile 9 01/12/06
180°
160° W
140° W
120° W
100° W
80° W
0
100
200
300
400
260
240
240
240
Profile 17 03/15/06
180°
160° W
140° W
120° W
100° W
80° W

Figure 18

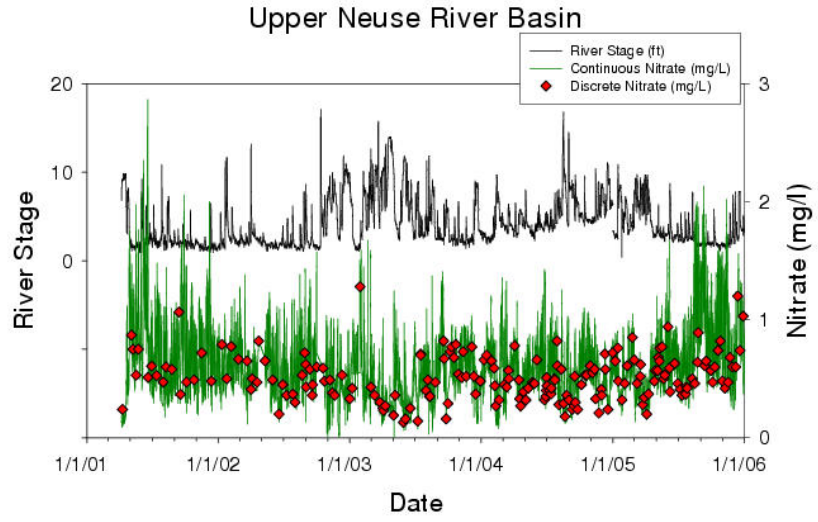
Upper Neuse River Basin
River Stage (ft)
Continuous Nitrate (mg/L)
Discrete Nitrate (mg/L)
River Stage
Nitrate (mg/l)
20
10
0
3
2
1
0
1/1/01
1/1/02
1/1/03
1/1/04
1/1/05
1/1/06
Date

A

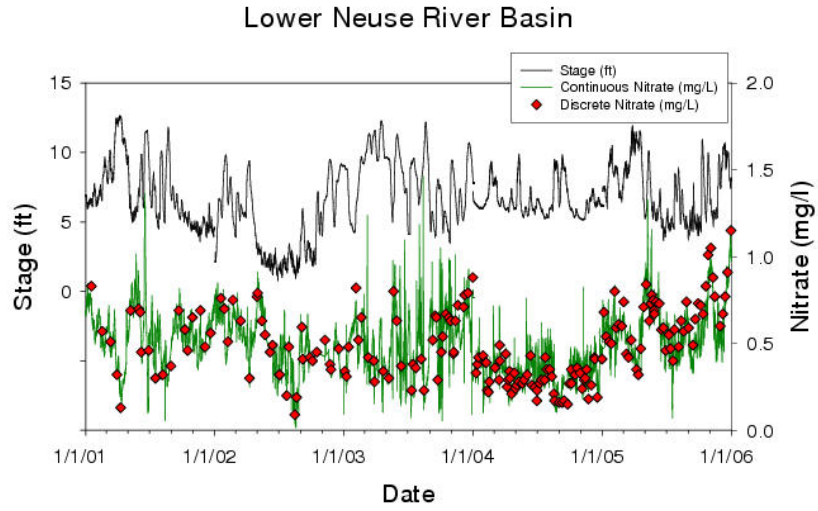
Lower Neuse River Basin
Stage (ft)
Continuous Nitrate (mg/L)
Discrete Nitrate (mg/L)
Stage (ft)
Nitrate (mg/l)
15
10
5
0
2.0
1.5
1.0
0.5
0.0
1/1/01
1/1/02
1/1/03
1/1/04
1/1/05
1/1/06
Date

B

Figure 19

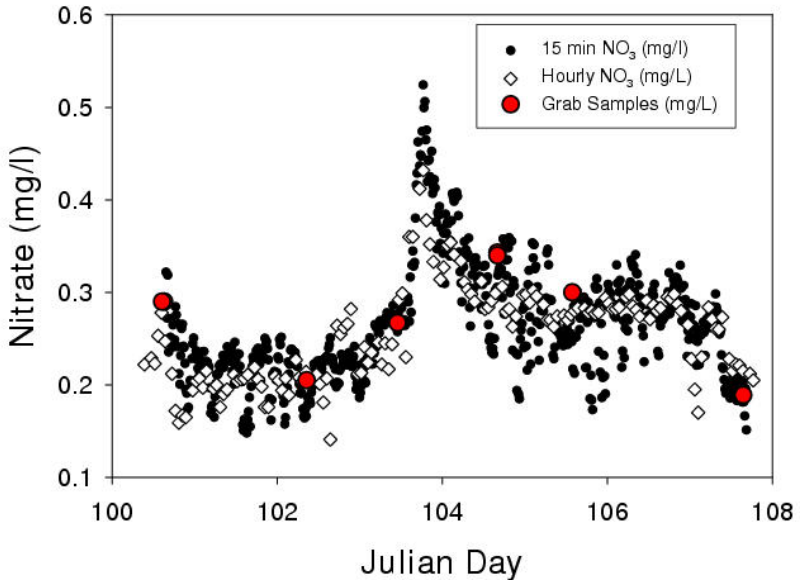
15 min NO3 (mg/l)
Hourly NO3 (mg/L)
Grab Samples (mg/L)
Nitrate (mg/l)
0.6
0.5
0.4
0.3
0.2
0.1
100
102
104
106
108
Julian Day

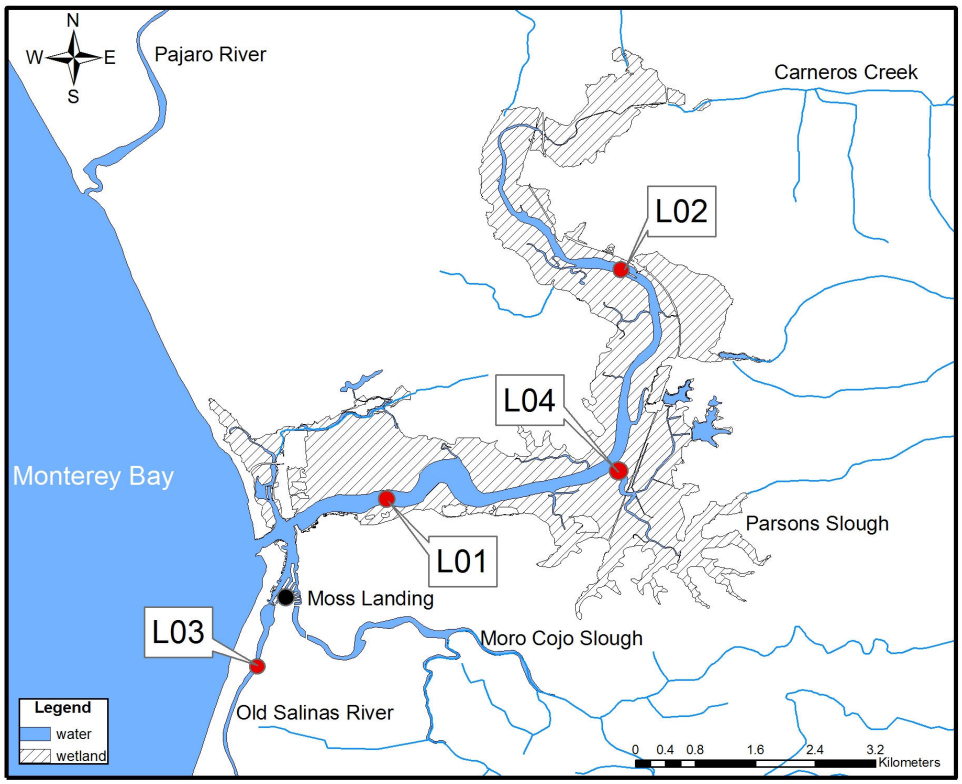
N
W
E
S
Pajaro River
Carneros Creek
L02
L04
Monterey Bay
Parsons Slough
L01
Moss Landing
L03
Moro Cojo Slough
Old Salinas River
Legend
water
wetland
0 0.4 0.8 1.6 2.4 3.2
Kilometers

Figure 20.

Figure 21

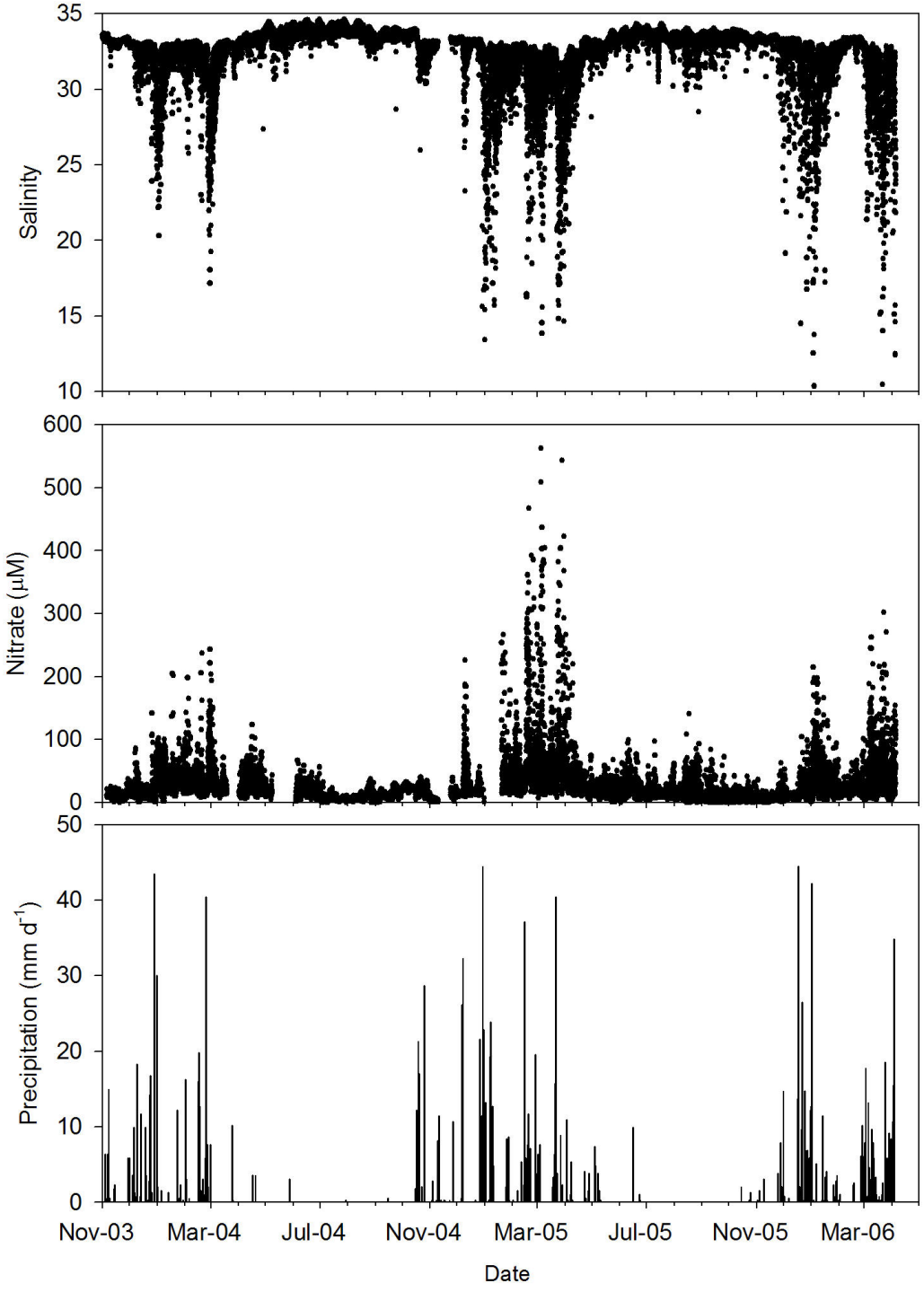
Salinity
35
30
25
20
15
10
Nitrate (µM)
600
500
400
300
200
100
0
Precipitation (mm d-1)
50
40
30
20
10
0
Nov-03
Mar-04
Jul-04
Nov-04
Mar-05
Jul-05
Nov-05
Mar-06
Date

Figure 22

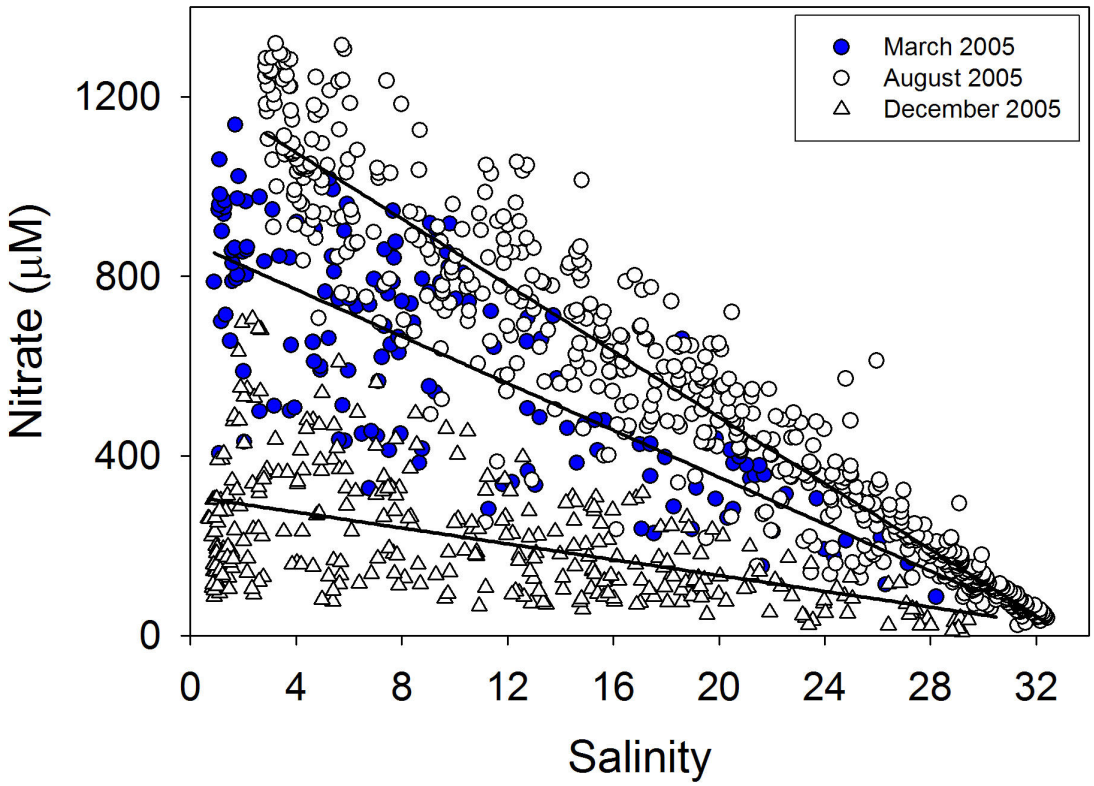
March 2005
August 2005
December 2005
Nitrate (µM)
1200
800
400
0
0
4
8
12
16
20
24
28
32
Salinity

Figure 23

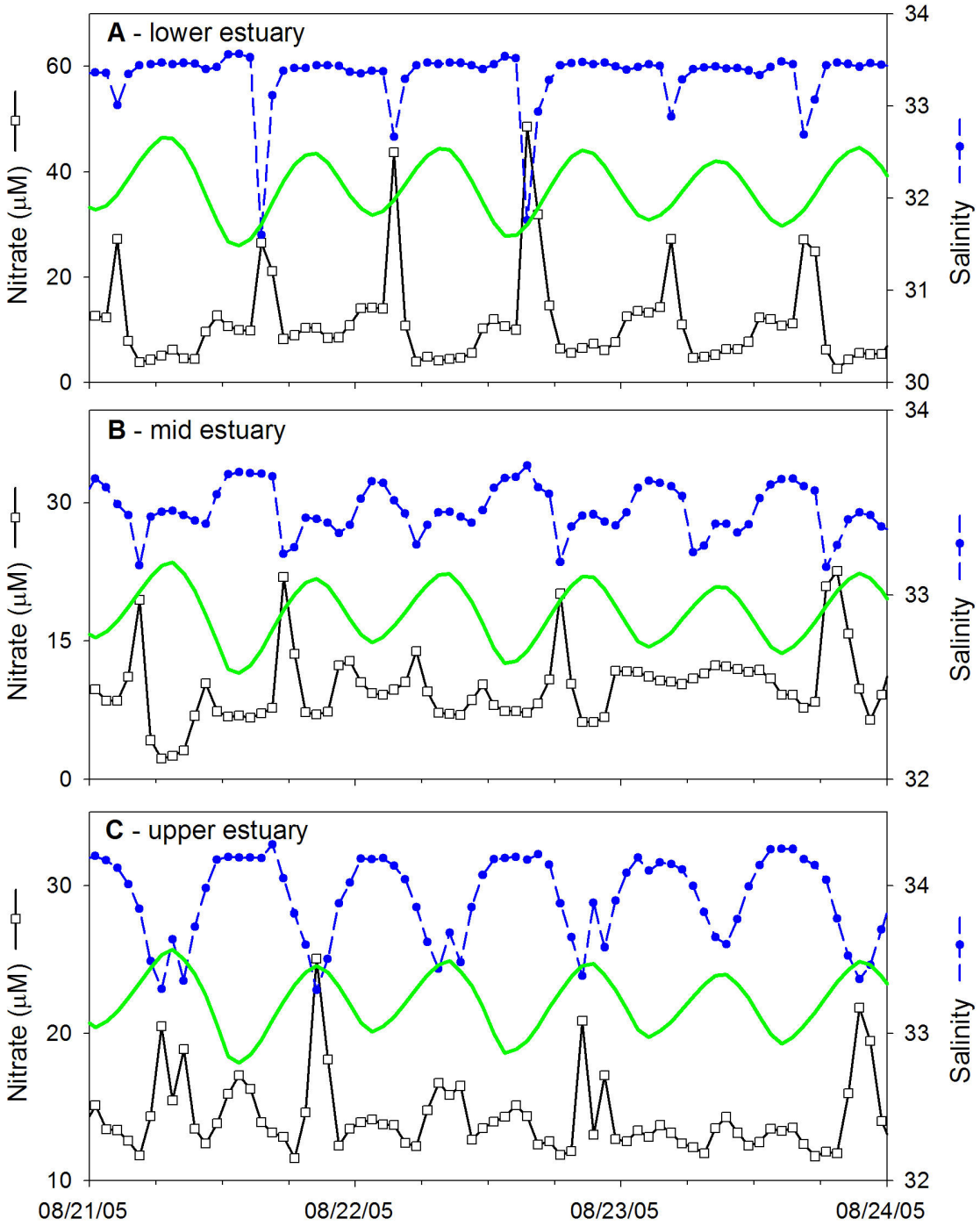
A - lower estuary
B - mid estuary
C - upper estuary
Nitrate (µM)
Salinity
08/21/05
08/22/05
08/23/05
08/24/05

Figure 24

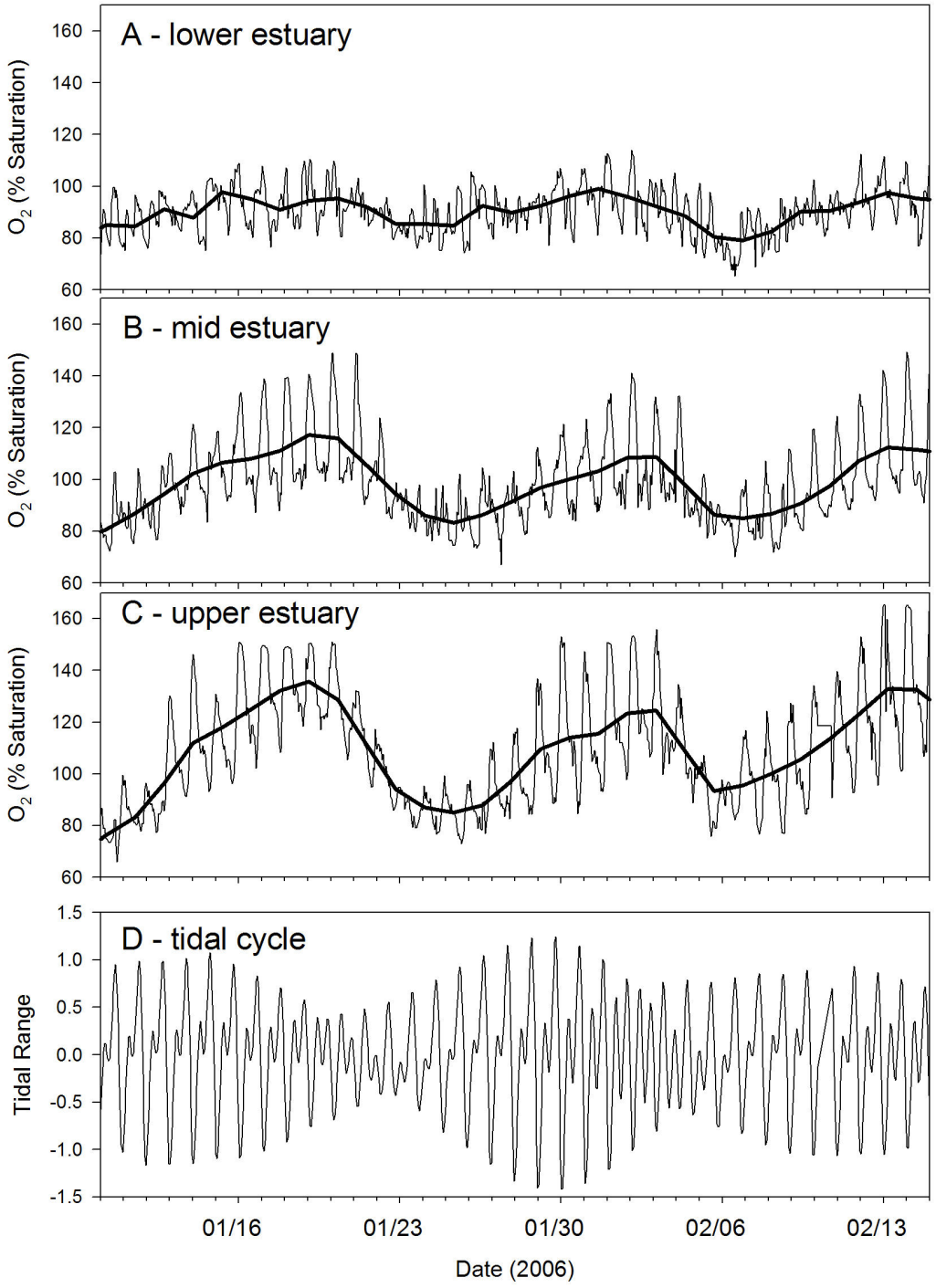
A - lower estuary
B - mid estuary
C - upper estuary
D - tidal cycle
O2 (% Saturation)
Tidal Range
160
140
120
100
80
60
1.5
1.0
0.5
0.0
-0.5
-1.0
-1.5
01/16
01/23
01/30
02/06
02/13
Date (2006)